

# Towards Causality-Aware Inferring: A Sequential Discriminative Approach for Medical Automatic Diagnosis

Junfan Lin<sup>a</sup>, Keze Wang<sup>a,\*</sup>, Ziliang Chen, Xiaodan Liang<sup>b</sup>, Liang Lin<sup>a</sup>

<sup>a</sup>the School of Computer Science and Engineering, Sun Yat-sen University, Guangzhou, China, 510006.

<sup>b</sup>the School of Intelligent Systems Engineering, Sun Yat-sen University, Guangzhou, China, 510006.

---

## Abstract

Through learning from the patient simulator built on the collected patient-doctor dialogues records, medical automatic diagnosis (MAD) aims to build an interactive diagnostic agent to sequentially inquire about symptoms for discriminating diseases. However, due to some task-unrelated and non-causal associations in these collected data, e.g., the preference of the collectors, the simulator is probably biased against the disease-symptom causality and the diagnostic agent might be hindered from capturing the transportable knowledge. This work attempts to address these critical issues in MAD by taking advantage of the structural causal model (SCM) to identify and resolve two representative non-causal biases, i.e., (i) default-answer bias and (ii) distributional inquiry bias, from the aspects of the data usage and the agent design, respectively. Specifically, Bias (i) originates from that the patient simulator tries to answer unrecorded inquiries with default answers, which cannot be resolved by feeding more data [1]. Suffering from the biased simulator, previous MAD methods cannot fully demonstrate their advantages. To eliminate this bias and inspired by the propensity score matching technique with SCM, we propose a propensity-based patient simulator to effectively answer unrecorded inquiry by drawing knowledge from the other records; Bias (ii) inherently comes along with the passive manner of collecting MAD data, and is one of the key obstacles for training the agent towards “learning how” rather than “remembering what”. For example, if a symptom is highly coupled with a certain disease within the training distribution, the agent might learn to only inquire about that symptom to discriminate that disease, and might not generalize to the out-of-distribution cases. To this end, we propose a progressive assurance agent, which includes the dual processes accounting for symptom inquiry and disease diagnosis. The inquiry process is driven by the diagnosis process in a top-down manner to inquire about symptoms for enhancing diagnostic confidence. The diagnosis process can picture the patient mentally and probabilistically, and further reasons within that mental representation by intervening with imaginary questions like “What if the patient coughs?”. By intervention, our proposed agent diagnoses according to the existence of symptoms instead of the inquiry pattern to eliminate the distributional inquiry bias. Extensive and comprehensive experiments demonstrate that our proposed framework achieves new state-of-the-art performance and possesses the advantage of transportability. The source code is available at <https://github.com/junfanlin/CAMAD>.

*Keywords:* causal inference, medical automatic diagnosis, transportability, sequential discriminative decision making, reinforcement learning

---

## 1. Introduction

The purpose of medical automatic diagnosis (MAD) is to learn an agent to sequentially interact with the patient, for symptom information collecting and preliminary diagnosing. Due to its huge industrial potential, this task has attracted the increasing attention of researchers [2, 3, 4, 5]. Similar to other task-oriented dialogue tasks, e.g., movie ticket/restaurant booking, online shopping, and technical support [6, 7, 8], MAD is composed of a series of dialogue-based interactions between the user and the agent, which can be formulated as a Markov decision process and re-

solved by deep reinforcement learning (RL) [3, 4]. However, unlike the video games [9, 10] or board games [11, 12] that have grounded simulators for RL agents to conduct substantial trial-and-error interactions, many real-world tasks like MAD only have passive observational data collected in real-world scenarios, such as the diagnosis dialogue records that happened between patients and doctors. Therefore, to apply RL to MAD, building a simulator using the passive observational data collected in the real world has been proposed as a promising workaround [4, 3, 13, 14]. Unfortunately, these passive data are inevitably biased by the non-causal and task-unrelated factors, such as the preference of the collectors and the distribution of the participants. Learning RL agents without mitigating these biases would hamper the agent to discover the causal and transportable skills of interest behind the data.

In this paper, we discover two representative non-causal associative biases neglected by previous MAD studies,

---

\*Corresponding author

Email addresses: [linjf8@mail12.sysu.edu.cn](mailto:linjf8@mail12.sysu.edu.cn) (Junfan Lin), [kezewang@gmail.com](mailto:kezewang@gmail.com) (Keze Wang), [c.ziliang@yahoo.com](mailto:c.ziliang@yahoo.com) (Ziliang Chen), [xdliang328@gmail.com](mailto:xdliang328@gmail.com) (Xiaodan Liang), [linliang@ieee.org](mailto:linliang@ieee.org) (Liang Lin)

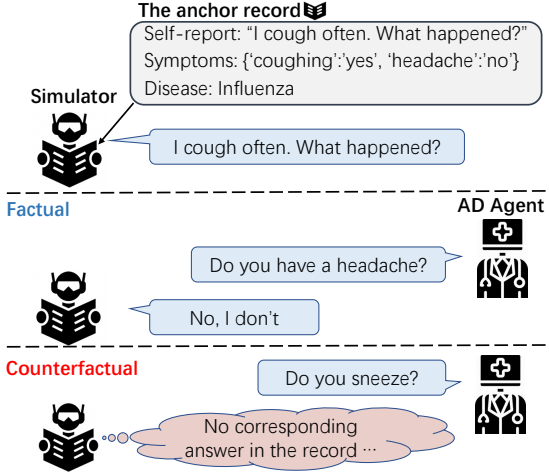


Figure 1: The demonstration of the counterfactual symptom inquiry problem. The patient simulator chooses a record as the anchor record and gives its self-report to start a diagnosis process. Then, the simulator answers the *factual symptom inquiries* which are already observed in the anchor record. This simulator would fail to answer the *counterfactual symptom inquiries* about the unobserved symptoms.

from the perspectives of the usage of passive data and the design of the diagnostic agent. According to the source of these biases, we denote them as *default-answer bias* and *distributional inquiry bias*, respectively.

**Default-answer bias.** During the data cleaning process in most tasks, setting default values is common to address the missing value problem [15]. In MAD, previous methods [4, 3] also adopt a patient simulator using the *default answer* for the unrecorded symptom inquiries. Specifically, this simulator chooses a dialogue record (i.e., the anchor record) from the dialogue dataset, and then answers the inquiry from the agent by looking the inquiry up in the anchor record. However, since the passive record only reflects one side of the world (i.e., the *factual* aspect), the simulator that trivially looks up in the factual data might fail to answer the unrecorded inquiries (i.e., the *counterfactual* aspects) from the RL agent, as exemplified in Fig. 1. To deal with the counterfactual inquiries, prior works [4, 3] simply make the simulator render ‘not sure’ responses as the default answers. However, considering that MAD is an interactive task, such strategy in fact brings about the collider bias [1] revealed by the structural causal model (SCM) among the symptom, inquiry, and answer (Fig. 2). By convention, *observation* (i.e., answer) is the common outcome of *symptom* and *inquiry*. In Fig. 2, those causal diagrams bounded by the solid box illustrate that the status of the symptom can be any value agnostic to the status of the inquiry. However, in the dashed box, the non-inquired observation is controlled as “not sure”, and the possible statuses of the symptom become related to the status of the inquiry. Especially, when inquired, there is only one possible status of the symptom in these controlled diagrams, i.e., “not sure”. For intuitive understanding, the simulator using the default answer simply assumes that if the patient is not inquired about a symptom, the patient should have been not sure about that symp-

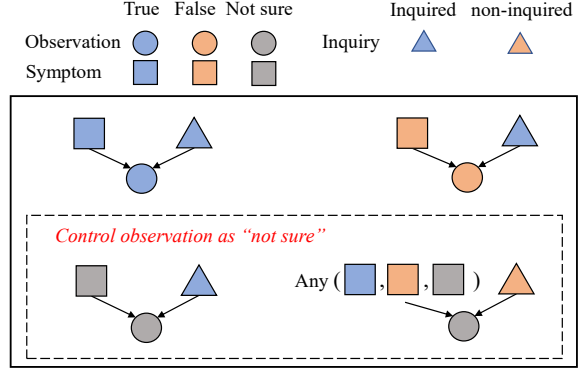


Figure 2: The causal diagram among the symptom, observation, and inquiry. Causally (boxed by solid line), the status of the symptom is independent of the status of the inquiry. However, when the observation is controlled as “not sure” (boxed by dashed line), the status of symptom is dependent on the status of the inquiry, which probably introduces the collider bias [1].

tom, which might deviate from reality. Learning with this collider bias hampers the agent to access the causal relationship between symptoms and diseases. Unfortunately, the collider bias cannot be eliminated by boosting with more training data [1]. What’s worse, due to the sparsity of the information in MAD, the simulator will be frequently inquired about unrecorded symptoms during the training phase, which further amplifies the negative impact of the collider bias. Training and evaluating under the simulator with severe collider bias cannot fully reflect the advantages of the diagnostic agent.

As a matter of fact, the simulator should infer the symptom ignorant of the inquiry and render the answer accordingly rather than providing the default answer to the counterfactual inquiry. To provide such ‘ignorability’ [16, 17], we propose a propensity-based patient simulator (PBPS) by leveraging the well-known causal inference technique, i.e., *Propensity Score Matching* (PSM) [18, 19, 20] from the potential outcome framework (PO). Our proposed simulator takes the novel step towards combining the different causality concepts of both SCM and PO frameworks to resolve practical problems. Usually, the comprehensive SCMs are unknown in real-world tasks like MAD, due to the unobserved factors such as individual effect. PO allows our simulator to perform causal inference focusing on the specific issues revealed by a partial SCM. Concretely, for building a PBPS in MAD, we first identify the colliders (see Fig. 2) based on the partial SCM of the passive data. Next, we employ PSM to calculate the propensity score of each record according to their symptoms and disease labels, and then group the records with similar propensity scores. Among the grouped records, the collider is decontrolled since the symptoms and diseases are matched except for the collider. Therefore, deducing the potential existences of the unobserved symptoms within these records can significantly reduce the collider bias.

**Distributional inquiry bias.** Another representative

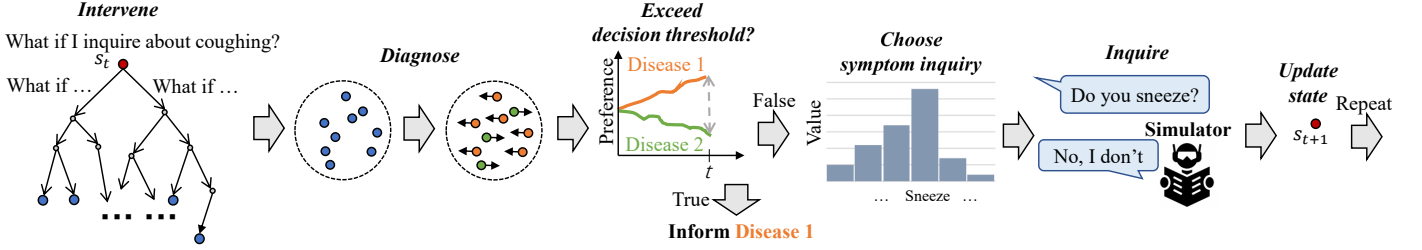


Figure 3: An example sketch of our P2A with binary disease alternatives. P2A conducts intervention to picture the complete patient and diagnose for all possible imagining patients. After, it estimates the timely confidence of the two disease candidates. Once the confidence gap between two alternatives exceeds the decision threshold, the winner with higher confidence will be executed. Otherwise, P2A continues inquiring about symptoms to collect more evidence.

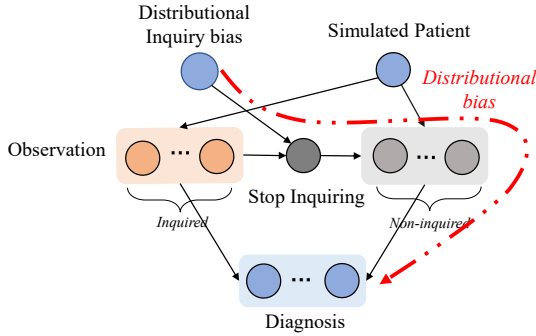


Figure 4: The causal diagram for the diagnostic agent. The distributinal inquiry bias misleads the agent to stop inquiry with insufficient symptom observation. Consequently, the collected data is always homogeneous and insufficient. The diagnoser learned with these data tends to overfit and is hard to generalize to other more complex scenarios.

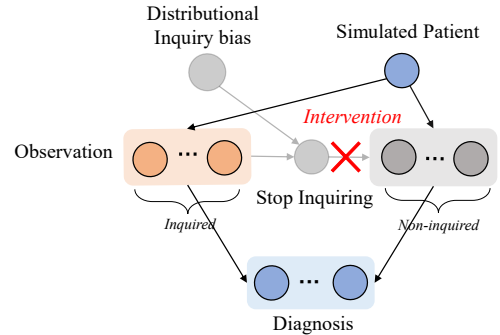


Figure 5: Eliminating the distributinal bias via intervention.

bias that comes along with passive data is the distributinal bias, which is also one of the key obstacles for training the agent towards “learning how” rather than “remembering what”. Due to the difficulty and high cost of collecting MAD data, the diagnostic agent suffers from the scarcity of training data and might be fragile to the out-of-distributinal cases. Specifically, we find that the distributinal bias of data might flow into the disease diagnosis through the inquiry behavior of the diagnostic agent, and we name such kind of bias as the *distributinal inquiry bias*, as depicted in Fig. 4. As a reminder, the diagnostic agent inquires about a series of symptom inquiries sequentially for the final discriminative diagnosis. The inquiry behavior acts like a window that controls the amount of information from the patient to the diagnosis. In this manner, when the given information for learning is not comprehensive, e.g., the diseases are highly coupled with a small set of symptoms, the agent might trivially associate these insufficient symptoms with the disease. Hence, once the requirement of symptom inquiries alters (e.g., changing the distribution of the patients), the agent might not be able to transport the knowledge to handle these out-of-distribution cases.

To this end, we propose a neuro-inspired progressive assurance agent (P2A) according to the revealed SCM

(Fig. 4). P2A is a dual-process agent, consisting of two separate yet cooperative branches, i.e., the diagnosis branch and the inquiry branch. As exemplified in Fig. 3, the diagnosis branch first reasons and plans according to historical observations (namely,  $s_t$  in the figure) by intervening in the unknown aspects of the patient. Such intervention results in diverse imaginary future scenarios. Then, these imagined trajectories are classified into different disease clusters. Once the population of one cluster is significantly overwhelming the others by a decision threshold [21], the agent will stop inquiring and the corresponding disease of that cluster will be informed. Different from the prior works [3, 4] that end the process through black-box policy networks, our P2A’s stop mechanism is more reliable and interpretable, thanks to that the competitive behavior and the concept of the decision threshold of our P2A are all derived from the diffusion model in neuroscience [21]. Not limited to the binary-alternatives case in neuroscience, our P2A has extended the diffusion model to a multi-alternatives setting from a computational perspective. By intervention, the diagnostic decision in our P2A is not only made according to the limited historical observations affected by the distributinal inquiry behavior but also is determined by the imagined completed patient information. As shown in Fig. 5, our P2A intervenes in the non-inquired observations by reducing their causes to the outcomes of the patients. Thus, the distributinal inquiry bias to the diagnosis is eliminated. The diagnosis branch of our P2A also regulates the inquiry branch in a top-down

manner to collect symptom evidence for approaching the decision threshold rapidly.

It is noteworthy that, our P2A is not just a model that manages to reduce the distributional bias, but also an interdisciplinary approach, bringing together new ideas and advances in anthropology, causality, neuroscience, and machine learning. As many anthropologists [22, 23] point out, the decisive ingredients for humankind to achieve global domination is the ability to picture the environment mentally, reason within that mental representation, and intervene in it by imagination questions like “What if I open the box?”. J. Pearl and M. A., Hernán [24, 25] postulated that it’s critical to equip learning machines with causal reasoning tools to achieve accelerated learning speeds as well as human-level performance. There are other biological discoveries in neuroscience that, when making sequential discriminative decisions, there are dual processes [26] in the human brain with different functions. One of the representative perspectives is that a dual-process cognitive architecture focuses on the distinction between explicit and implicit cognitive processes [27]. The top-level is more rational and in pursuit of long-horizon values whereas the bottom-level is more emotional and sensitive to the time-discounted utility. Especially, the most recent “*as soon as possible*” effect [28] shows that the bottom-level is dependent on the reward as well as *getting something as soon as possible*, and is learned through gradual trial-and-error learning (e.g., reinforcement learning) [27].

Overall, the main contributions of our paper are tri-fold: i) We identify the default-answer bias existed in the patient simulator of prior works and present a novel patient simulator PBPS to tackle this problem, which may also inspire other RL tasks with passive observational data; ii) we also identify the distributional inquiry bias and propose a novel MAD agent P2A to eliminates the distributional bias via intervention; iii) unlike prior methods that end the interaction through a black-box policy network, P2A achieves more reliable and interpretable decision making by introducing a neuro-inspired ‘decision threshold’ to proactively determine when to stop discoursing. Considering the addressed causality issues, we name our framework, consisting of PBPS and P2A, as Causality-Aware MAD (CA-MAD). Experimental results demonstrate that: i) our PBPS is superior in answering counterfactual symptom inquiry and generating more informative and disease-related answers; ii) our P2A advances in capturing the symptom-disease relationship and generalizing it to out-of-distribution cases, and also possesses the advantage of sample-efficient and robustness, compared to other existing MAD methods.

The remainder of this paper is organized as follows. Section 2 comprehensively reviews the related works and the existing MAD methods based on RL. Section 3 presents the background of reinforcement learning, the identified causal issues, and the formulation of our CA-MAD framework. Section 4 presents the experimental results and human evaluation on two public MAD benchmarks with com-

prehensive evaluation protocols, as well as comparisons with the competitive alternatives. In Section 5, we discuss the limitation of our methods. Finally, Section 6 concludes this paper.

## 2. Related Work

Our propensity-based patient simulator and progressive assurance agent incorporate three key ingredients: the popular causal inference technique *propensity score matching* (PSM) [19, 20], user simulator in a dialogue system [13], and medical automatic diagnosis system [4, 3, 29] by means of reinforcement learning [9, 10]. In the field of causal inference, there are many different methods proposed in recent years, which can be approximately categorized into two branches according to whether the causal relationship is modeled explicitly or implicitly, namely, the structural causal model (SCM) framework [30] and the potential outcome framework [16]. The methods based on the SCM usually incorporate a causal diagram (with the form of a Bayesian model) and structural causal equations [31]. Then, the collected data are injected into the model to infer the causal effect. Recently, many approaches based on the causal model have been proposed in computer vision [32, 33, 34, 35, 36], reinforcement learning [37, 38, 39], etc. Most of these works are based on the general causal model for the population. However, in MAD, patients with the same diseases may have different symptoms due to individual differences. To model such individual-level relation, the structural causal diagram can include individual information into the diagram [40]. Moreover, the model-free causal inference framework (i.e., the potential outcome framework [16] (PO)) infers the causal effect from passive observational data without an explicit causal model and it’s also capable of handling individual causal effects. In our paper, we combine the both merits of the SCM’s interpretability and PO’s model-free to tackle practical problems.

In the context of medical automatic diagnosis, the collected dialogue records are passively observed, that’s, the existence of the unobserved symptoms is *missing* [41]. Inferring the existence of the unobserved symptoms is non-trivial, particularly if the inference is association ignorant of the causal relationship [40]. The biases are often introduced when there are either uncontrolled confounders [30] or controlled colliders [1]. These biases usually cannot be solved by boosting with more data [42]. To eliminate these biases, there are many mature causal inference techniques, e.g., two-stage least squares [43], backdoor adjustment [42, 44, 18], etc. The identified counterfactual symptom inquiry problem in this work is due to the collider biases. One solution to eliminate the collider biases is to block off the influence path to the colliders by providing the ignorability [17, 16]. Such ignorability can be obtained through matching techniques [45]. In MAD, the collected data are usually very sparse therefore ordinary matching methods are usually infeasible due to the problem of *lack of*

*overlap*. To resolve this problem, propensity score matching (PSM) [18, 20] is introduced to estimate the propensity of the instance for matching, which is a low-dimension but compact representation.

Related to our simulator, current works [3, 4] also proposed to build patient simulators on the collected data. However, their patient simulators overlook the importance of incorporating the causal relationship. In specificity, they adopt patient-doctor conversation records [46, 47] to generate responses, which typically lack the symptom complexity of human interlocutors, and the trained agent is inevitably affected by biases in the design of the simulator [48]. To fill in missing data, [13] incorporated a model of the environment into the dialogue agent to generate a simulated user experience, which however is prone to generate data with similar characteristics as the original data [14]. A reinforced agent who takes actions to explore might receive a false response from the simulator as the simulator only knows how to answer according to what is in the record.

As for the task-oriented dialogue agent, most of the current task-oriented dialogue systems adopt the framework of reinforcement learning (RL) [10, 6, 49], and some works [50, 51, 52] adopt the sequence-to-sequence style for dialogue generation. For medical dialogue systems, due to a large number of symptoms, reinforcement learning is a better choice for topic selection [2, 53, 29]. Deep reinforcement learning has reaped great success because of its good capacity of rich value function approximators [11, 10, 54]. According to the type of action space, current RL methods can be divided into two classes, namely, discrete control [9] and continuous control [55]. In the context of medical automatic diagnosis, the actions of symptom inquiry and disease diagnosis are discrete. Therefore, most of the current MAD methods exploit the classical discrete control methods, e.g., Deep Q-Network (DQN) [10] to select the actions. [2] applied DQN to diagnose using synthetic data. While [4] first did experiments on real-world data using DQN. To include explicit medical inductive bias for improving the diagnostic performance, KR-DQN [3] proposed an end-to-end model guided by symptom-disease knowledge priors. KR-DQN applies the predefined conditional probability of symptom and disease to transform the Q-values estimated by DQN. Moreover, most of these methods integrate symptom-inquiry and disease-diagnosis actions into one single reinforced policy network without considering the essential difference between symptom-inquiry and disease-diagnosis such as the internal relationships among the inquired symptoms, non-inquired symptoms as well as disease candidates. Differently, our work follows the logic of MAD in real life and formulates it as a sequential discriminative decision-making problem. Sequential discriminative decision making is a natural cognitive process found in human’s daily rational and economic decisions [56], such as eye gazing [57] and product selection [58]. In the studies of neuroeconomics, researchers establish a dual-process theory [59, 60, 61] to

explain the neuro-spiking pattern [62] in the human brain when making an economic and rational decision. To model the decision-making process, neuroeconomics proposes a diffusion model [63]. Specifically, in the diffusion model, the decision is made according to the difference of accumulating neuro-spiking ratios between binary alternatives. And once the difference exceeds the decision threshold, the winner decision will be made. Inspired by these discoveries, our proposed dual-process P2A also incorporates the concept of decision threshold for the diagnoser to determine when to inform disease. Moreover, our method extends the binary-alternatives settings in neuroscience to multi-alternatives setting computationally. Like ours, PG-MI-GAN [5] adopts a separate diagnoser from the inquiry policy. Specifically, it trains an inquiry generator to generate a sequence of inquiries indistinguishable by the discriminator, and further uses a pretrained diagnoser to finetune the generator. As we discovered, the design of the diagnoser needs to take the indirect bias [64], distributional bias [65, 66, 67, 68] as well as training bias [69] into account to better capture the symptom-disease relationship and improve the *transportability* [70] of the diagnosis agent.

Moreover, as a medical application, a MAD agent is also required to consider the uncertainty of its decision to provide a robust and trustful diagnosis result for the ethics concern. Most of the current MAD agent is allowed to jump into informing a disease without any regulation. Instead, our MAD agent takes the uncertainty to augment the decision-making process. There are plenty of works studying how to combine uncertainty and exploration [71, 72, 69, 73, 74]. However, different from ours, these works do not employ uncertainty to provide a stop mechanism for sequential decision making.

### 3. Causality-Aware MAD

#### 3.1. Preliminaries

As shown in Fig. 1, a diagnosis record consists of a self-report, symptom existences  $\mathbf{y} = [y_a]_{a=1}^n \in \{-1, 0, 1\}^n$  (-1 for ‘no’, 0 for ‘not sure’, 1 for ‘yes’), and a ground-truth disease label  $d \in [1, m]$ , where  $n$  is the number of symptoms and  $m$  is the number of diseases. An example record is depicted as Fig. 2 in Appendix.

**Reinforcement learning.** The MAD task is usually formulated as a Markov decision process (MDP) problem [4, 3], and is denoted by the tuple  $\mathcal{M} = \{\mathcal{S}, \mathcal{A}, \mathcal{P}, \mathcal{R}, \gamma\}$ .  $\mathcal{S} \subseteq \mathbb{R}^n$  denotes the state space, in which,  $\mathbf{s}_t \in \mathcal{S}$  maintains the values of all mentioned symptoms (i.e., -2 for non-inquired symptom, -1 for ‘no’, 0 for ‘not sure’ and 1 for ‘yes’) up to time  $t$ .  $\mathcal{A} \subseteq \mathbb{N}^{n+m}$  represents the action space of the agent, in which  $a \in \mathcal{A}$  is either the symptom inquiry or disease diagnosis.  $\mathcal{R} : \mathcal{S} \times \mathcal{A} \rightarrow \mathbb{R}$  is the reward function that measures the diagnosis progress.  $\mathcal{P} : \mathcal{S} \times \mathcal{A} \rightarrow \mathcal{S}$  is the transition dynamics. The target of reinforcement learning is to solve via a policy form

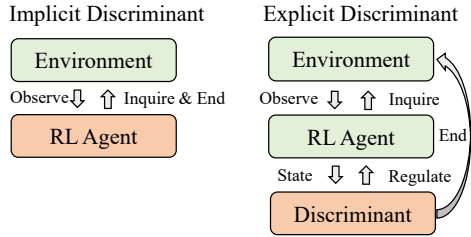


Figure 6: Left: Fusing both inquiry and discriminant implicitly by reinforcement learning; right: Disentangling inquiry and discriminant via reinforcement learning and discriminative learning respectively.

$\pi : \mathcal{S} \rightarrow \mathcal{A}$ , which maximizes the expected sum of rewards:  $\eta(\pi) = \mathbb{E}_{\pi, \mathcal{M}}[\sum_{t=0}^T \gamma^t \mathcal{R}(s_t, a_t)]$  ( $T$  is the ended timestep).  $\gamma \in [0, 1]$  is a discount factor. The initial state  $s_0$  is initialized by the symptoms mentioned in the self-report (also named as explicit symptoms). The most distinction between MAD and classical RL tasks (e.g., Atari 2600 [9] and MuJoCo [75]) is that a MAD agent needs to proactively decide when to terminate the trajectory by informing the final diagnosis. Conventionally, the symptoms in this task are regarded as the causes of the answers of the patients, which makes the task solvable from the perspective of causality.

### 3.2. Sequential discriminative decision making.

Unlike priors [4, 3] that fuse inquiry and discriminant into a black-box neural network learning via RL, our paper poses it as a sequential discriminative decision-making problem. Fig. 6 depicts the difference between the priors (left) and ours (right). Specifically, we adopt an RL agent as the interface between environment and discriminant. Then, the RL agent inquires about information (observation) from the environment and summarized the observations as a state for the discriminant. The discriminant component is responsible for ending the interaction by informing the discriminative decision proactively. In this manner, our proposed diagnostic agent is capable of comprising dual processes for inquiry and discriminant, respectively.

### 3.3. Causal Issues and Solutions

**Default-answer bias:** To build a patient simulator, a diagnosis record is employed to demonstrate how to answer the agent’s symptom inquiry  $a$ . In the given record, the simulator can access both the symptom existences  $\mathbf{y}$  and the disease label  $d$ . Furthermore, the simulator can answer a factual symptom inquiry, while failing to answer a counterfactual symptom inquiry unobserved in the record, as demonstrated in Fig. 1. The structured equation model (SEM)<sup>1</sup> of the diagram in Fig. 2 is:

<sup>1</sup>For simplicity, we don’t enumerate all variables such as noise variables in our SEMs since we don’t calculate them explicitly in either PBPS or P2A.

- (i) Inquiry, symptom  $\rightarrow$  observation (for each symptom)

SEM (i) denotes that the observation for each symptom is caused by symptom and inquiry. According to SEM (i), there will be a non-causal association between ‘Inquiry’ and ‘Symptom’ if their collider, i.e., non-inquired ‘Observation’, is controlled. For instance, the vanilla patient simulator can only answer the counterfactual symptom inquiry with ‘not sure’ because it controls the ‘Inquiry’ node of the unobserved symptom as ‘non-inquired’. To infer the non-inquired symptom causally, the most straightforward solution is to decontrol the collider, that’s, the non-inquired observation. To achieve this, we resort to matching [45] to gather records that have similar covariates except for the inquiries of the non-inquired observations. By this means, the non-inquired observation is various among the matched records.

However, the covariates of a MAD record (e.g., the inquired observations) are severely sparse, making the samples terribly difficult to match. To resolve this *lack of overlap* issue, propensity score matching (PSM) [18, 19, 20] is developed to estimate an equivalent while more compact representation for matching, i.e., the propensity score  $P(\text{action}|\text{covariates})$ . As mathematically explained in Appendix A.1, given the same propensity score, the aforementioned ignorability still holds, and therefore PSM blocks off the influence path from ‘Inquiry’ to ‘Symptom’. In the MAD task, given a record with covariates  $(\mathbf{y}, d)$ , the propensity score is  $P(A|\mathbf{y}, d)$ , where  $A$  is the factual symptom inquiry. In our paper, we not only require the propensity w.r.t. inquiry to be matched but also require the propensity w.r.t. symptom to be matched. Therefore, instead of  $P(A|\mathbf{y}, d)$ , we adopt a more strict propensity score that also takes the existences of the inquired symptoms into account, that’s,  $P(Y_a|\mathbf{y}, d)$ , where  $a$  is a symptom inquiry and  $Y_a$  is the existence of the inquired symptom. Please refer to Appendix A.2 for more mathematical explanations. Assuming symptoms are solely dependent on both the disease and the observed symptoms, the propensity score with all symptom inquiries is  $P(\mathbf{Y}|\mathbf{y}, d) = \prod_a P(Y_a|\mathbf{y}, d)$ .

**Distributional inquiry bias:** As discussed in the introduction section, distributional inquiry bias causes the agent to stop to inform disease before inquiring about sufficient symptoms, as depicted in Fig. 4, with the following SEMs:

- (ii) Simulated patient  $\rightarrow$  inquired observations
- (iii) Distributional inquiry bias, inquired observations  $\rightarrow$  stop inquiring
- (iv) Simulated patient, stop inquiring  $\rightarrow$  non-inquired observations
- (v) All observations  $\rightarrow$  diagnosis

According to the above SEMs, the ‘stop inquiring’ in SEM (iv) should be removed for the diagnoser to diagnose only according to the information from the simulated

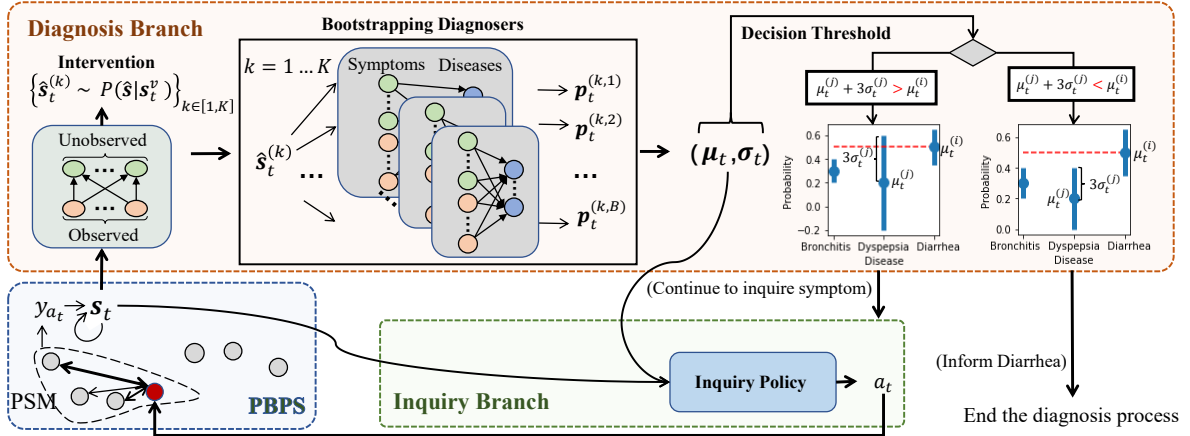


Figure 7: An overview of our CA-MAD. The diagnosis branch takes  $s_t$  to draw  $K$  final states which are fed into the  $B$  bootstrapping diagnosers to obtain the expectation and deviation. P2A keeps inquiring about symptoms of the patient simulator until the diagnosis meets the decision threshold.

patient. To achieve this objective, we take advantage of the intervention to block the effect path from stop inquiring to non-inquired observation. Formally, interventions are defined through a mathematical operator  $\text{do}(x)$  [76], which simulates physical interventions by deleting certain functions from the model, replacing them with a constant  $X = x$ , while keeping the rest of the model unchanged [76]. In our SCM, to delete the function of ‘Stop inquiring’, we use  $\text{do}(\text{Causes of non-inquired observations} = \text{simulated patient})$ .

These operations reduce our SCM from Fig. 4 into Fig. 5 with the following SEMs:

- (vi) Simulated patient  $\rightarrow$  inquired observations
- (vii) Simulated patient  $\rightarrow$  non-inquired observations
- (viii) All observations  $\rightarrow$  diagnosis

The diagnoser learned with this reduced SCM focuses on diagnoses according to the information from the patient. To achieve intervention, the diagnosis agent could infer the simulated patient from its inquired observations according to SEM (vi). The non-inquired observations can be determined given the simulated patient according to SEM (vii). Furthermore, the agent uses both inquired and estimated non-inquired observations to diagnose according to SEM (viii).

### 3.4. Formulation

Attempting to address these two representative biases, we propose our CA-MAD, which is comprised of the propensity-based patient simulator (PBPS) and the progressive assurance agent (P2A). The overview of the interaction between PBPS and P2A is shown in Fig. 7.

#### 3.4.1. Propensity-based Patient Simulator

**Propensity score modeling:** As introduced in the previous section, PSM aims to block off the influence path from ‘Inquiry’ to non-inquired ‘Symptom’ in Fig. 2,

---

### Algorithm 1 Propensity-based patient simulator (PBPS): $\mathcal{P}_{\text{PBPS}}(s_t, a_t; p)$

---

**Input:**  $s_t, a_t$ , anchor record  $p$ , self-report, and  $(y^{(p)}, d^{(p)})$   
**Output:**  $s_{t+1}$

- 1: **if**  $t = -1$  **then**
- 2:   Initialize  $s_0 \leftarrow [-2, -2, \dots, -2]$  with the size of  $n$ ,
- 3:   Let  $s_{0,a} \leftarrow y_a$ , for each  $a$  parsed from the self-report
- 4:   Return  $s_0$
- 5: **else**
- 6:   Initialize  $a \leftarrow a_t, s_{t+1} \leftarrow s_t, q' \leftarrow p$
- 7:   **If**  $((y_a = 0) \wedge (s_{t+1,a} = -2))$ , **sample**  $q' \sim P(q|p, a)$  **according to Equ.(2)**.
- 8:   Update state  $s_{t+1}$  by  $s_{t+1,a} \leftarrow y_a^{(q')}$
- 9:   Return  $s_{t+1}$

---

to eliminate the collider biases. It’s achieved by matching the records with similar estimated propensity scores,  $P(\mathbf{Y}|\mathbf{y}, d)$ . Intuitively, the propensity score represents the propensity w.r.t. inquiry of the patient (e.g., likely to be inquired about sneezing but coughing). The propensity score matching is to match different patients with similar propensity. Consequently, these patients are likely to experience the same diagnosing process. In this sense, the diagnosing processes of these patients are exchangeable [77] and make no differences among these patients. Among these matched patients, the only external factor (i.e., inquiry) associated with the symptoms is excluded and the effects from the covariates to the symptoms become causal. Since the propensity score also represents the covariates (i.e.,  $\mathbf{y}, d$ ), the symptoms of the matched patients are similar.

We use multilayer perceptron (MLP)  $f_{\phi_P}(\cdot)$  to model  $P(\mathbf{Y}|\mathbf{y}, d)$ , where  $\phi_P$  denotes the parameter of the network, by reducing the cross-entropy loss  $\text{CE}(P(\mathbf{Y}), y) = -y \log P(y)$ . We deploy the self-supervised strategy to train the  $f_{\phi_P}(\cdot)$  to estimate the potential symptom existence  $Y_a$  of any symptom inquiry  $a$ . Specifically, we mask

off some of  $\mathbf{y}$  with binary mask  $\mathbf{m}^2$  and train  $f_{\phi_P}(\cdot)$  to reconstruct  $\mathbf{y}$ , given the masked  $\mathbf{y}$  and  $d$ . The reconstruction target is

$$\min_{\phi_P} \sum_{i=1}^N \sum_{a=1:n, y_a \neq 0} \sum_{\mathbf{m}} \text{CE}(f_{\phi_P}(\mathbf{y}^{(i)} \odot \mathbf{m}, d^{(i)})_a, y_a^{(i)}). \quad (1)$$

After training, we adopt the output of the second-to-last fully-connected layer as the propensity score,  $f_{\phi_P}(\cdot)$ , since its dimension is much smaller and information is more compact, in comparison to the last.

**Potential existence of symptoms estimation:** Given an anchor record  $p$ , we show how the simulator estimates the existence of an unobserved symptom  $a$ . Our simulator explores all records  $\{\dots, q, \dots\}$  that have the same disease (i.e.,  $d^{(q)} = d^{(p)}$ ) and also have  $a$  in their observed symptoms (i.e.,  $y_a^{(q)} \neq 0$ ). It eliminates the irrelevant information of the inquired symptom and disease. The similarity weight of a record  $q$  w.r.t.  $p$  is formulated as

$$P(q|p, a) \propto \mathbb{I}\left((d^{(q)} = d^{(p)}) \wedge (y_a^{(q)} \neq 0)\right) \times e^{-\frac{\|f_{\phi_P}^{(p)} - f_{\phi_P}^{(q)}\|^2}{\sigma^2}}, \quad (2)$$

where  $e^{-\frac{\|f_{\phi_P}^{(p)} - f_{\phi_P}^{(q)}\|^2}{\sigma^2}}$  denotes a non-parametric density kernel [78] ( $\sigma > 0$  indicates a standard deviation of the propensity scores). The similarity of propensity scores of the patient record  $q$  and  $p$  implies that the existences of symptoms of these records are more probably similar.  $\mathbb{I}(\cdot)$  is an indicator function that returns 1 if the propositional logic formula in the bracket is satisfied, otherwise returns 0. Then the patient simulator can sample a record  $q' \sim P(q|p, a)$ , and use its symptom existence  $y_a^{(q')}$  as the potential symptom existence of the anchor record. More details are in Appendix A and a numerical example is in Appendix D.

The MDP transition  $\mathcal{P}_{\text{PBPS}}$  of our patient simulator is concluded in Alg.1. In Alg.1, line 7 (highlighted in bold and italics) is the extra operation of our simulator compared to the original simulator  $\mathcal{P}_{\text{PS}}$ . Our PBPS would conduct PSM among all training records when the symptom inquiry is unobserved in the anchor record.

### 3.4.2. Progressive Assurance Agent

To address distributional inquiry bias, we propose a *Progressive Assurance Agent* (P2A) consisting of two separate yet cooperative branches for symptom inquiry and disease diagnosis, as shown in Fig. 7. In our P2A, the ‘fast but impulsive’ inquiry branch inquires about symptoms to get  $\mathbf{s}_t$  from PBPS to maximize the sum of rewards, while the ‘slow but rational’ diagnosis branch imagines and reasons

<sup>2</sup>The binary mask is generated according to the order of the symptoms in the dialogue record. To maintain the priorities of the symptom inquiries, an entry in the mask can be set to be 0 only if the entries of its subsequent symptoms in the record are set to be 0. In practice, given a record, we randomly select a mentioned symptom, and then mask off all subsequent symptoms.

---

### Algorithm 2 Progressive Assurance Agent (P2A)

**Input:** Initial policy  $\pi_\theta$ , target policy parameters  $\theta_{\text{targ}} = \theta$ , final state estimator parameters  $\phi_G$ ,  $B$  bootstrapping diagnosers parameters  $\phi_B$ , empty replay buffer  $\mathcal{D}_Q$  and records buffer  $\mathcal{D}_C$ .

- 1: **for** episode = 1, E **do**
- 2:   Get one anchor record  $p$  to obtain the initial state  $\mathbf{s}_0$  according to the self-report
- 3:   **for**  $t = 0, T$  **do**
- 4:     Sample the final states:  $\{\hat{\mathbf{s}}^{(k)} \sim f_{\phi_G}(\mathbf{s}_t), k \in [1, K]\}$
- 5:     Forward to bootstrapping diagnosers:  $\mathbb{P}_t = \{f_{\phi_B}(\hat{\mathbf{s}}^{(k), k \in [1, K]})\} = \{\mathbf{p}_t^{(k, b)}, k \in [1, K], b \in [1, B]\}$
- 6:     Calculate the statistics  $\boldsymbol{\mu}_t, \boldsymbol{\sigma}_t$  of  $\mathbb{P}_t$
- 7:     **if**  $(\epsilon < p \sim U(0, 1)) \wedge (t \neq T)$  **then**
- 8:       Inquire symptom:  $a_t = s \sim U\{1, N\}$  s.t.  $\mathbf{s}_{t, s} = -2$
- 9:     **else if**  $\text{DT}(\boldsymbol{\mu}_t, \boldsymbol{\sigma}_t) \vee (t = T)$  **then**
- 10:       Inform disease:  $a_t = (\max_i \mu_t^{(i)}) + N$  to end the diagnosis process
- 11:       Store records  $(\mathbf{s}_t, d^{(p)})$  in  $\mathcal{D}_C$  and then start a new episode
- 12:     **else**
- 13:       Request symptom:  $a_t = \max_a Q(\mathbf{s}_t, \boldsymbol{\mu}_t, a; \theta)$
- 14:       Interact with the patient simulator and update state  $\mathbf{s}_{t+1} = \mathcal{P}_{\text{PBPS}}(\mathbf{s}_t, a_t; p)$  according to Alg. 1
- 15:       Store transition  $(\mathbf{s}_{t-1}, \boldsymbol{\mu}_{t-1}, a_{t-1}, \mathbf{s}_t, \boldsymbol{\mu}_t)$  in  $\mathcal{D}_Q$
- 16:       **if** time to update **then**
- 17:         Sample mini-batch from  $\mathcal{D}_Q$  and update  $\theta$  and  $\theta_{\text{targ}}$  according to Equ. (8) and Equ. (9)
- 18:         Sample  $B$  mini-batches from  $\mathcal{D}_C$  with replacement to update  $\phi_G$  and  $\phi_B$  according to Equ. (3) and Equ. (4)

---

the future scenarios to robustly estimate the disease and its confidence per step until it’s confident enough (satisfying *Decision Threshold* [21]) to inform a disease. The inquiry branch is driven by the diagnosis branch to inquire about symptoms that increase the confidence in order to *meet decision threshold as soon as possible*. More details are provided in Appendix B and a numerical example is in Appendix D.

**Diagnosis Branch:** To eliminate the biases mentioned in Sec. 3.3, our P2A intervenes in the observation to be only the effect of the simulated patients. Specifically, our P2A first infers the possible final state of the simulated patient  $\hat{\mathbf{s}}_t$  according to the inquired observation  $\mathbf{s}_t^v$ , that’s,  $P(\hat{\mathbf{s}}_t | \mathbf{s}_t^v)$ . Then, our P2A intervenes in the observations of the non-inquired symptoms  $\mathbf{s}_t^u$  with the estimated simulated patient, i.e.,  $\text{do}(\mathbf{s}_t^u = \hat{\mathbf{s}}_t - \mathbf{s}_t^v)$  (Fig. 5). One can intuitively treat such intervention processes as “imagining and reasoning the future interactions to obtain a more comprehensive patient state to achieve a reliable diagnosis”. After that, our P2A feeds the inquired and intervened symptoms as input to the discriminative diagnoser  $P(d | \hat{\mathbf{s}}_t)$ . In total, the diagnoser of our P2A diagnoses by using the observed symptoms via  $P(d | \mathbf{s}_t^v) = \sum_{\hat{\mathbf{s}}_t} P(d | \hat{\mathbf{s}}_t) P(\hat{\mathbf{s}}_t | \mathbf{s}_t^v)$ . We train the intervener  $f_{\phi_G}(\cdot)$  and the discriminative diagnoser  $f_{\phi_B}(\cdot)$  for  $P(\hat{\mathbf{s}}_t | \mathbf{s}_t^v)$  and  $P(d | \hat{\mathbf{s}}_t)$ , respectively.

*Intervener.* Intervener aims at predicting the final

symptom state  $\hat{\mathbf{s}}$  from the current inquired state  $\mathbf{s}_t^v$ . Therefore, we model it as a generative problem.  $\phi_M$  is the parameter of the generator  $f_{\phi_G}(\cdot)$ , whose target is defined with cross-entropy:

$$\min_{\phi_G} \sum_{i=1}^N \sum_{a=1:n, s_{i,a} \neq -2} \sum_{\mathbf{m}} \text{CE}(f_{\phi_G}(\mathbf{s}_i \odot \mathbf{m})_a, s_{i,a}), \quad (3)$$

where  $\mathbf{m}$  is the binary mask constructed as Equ. (1), and the target for  $f_{\phi_G}$  is to recover the masked information. As shown in the overview (Fig. 7), the Monte Carlo sampling is applied by obeying the generative model  $f_{\phi_G}(\mathbf{s}_t)$  to sample  $K$  possible final states  $\{\hat{\mathbf{s}}^{(k)}\}_{k=1}^K$ . Note that, the inquired symptoms of  $\mathbf{s}_t^v$  remain the same in these final states.

After the intervention, the  $K$  imaginary final states are fed to the diagnoser  $f_{\phi_B}(\cdot)$  to check whether the decision threshold is met or not.

*Decision Threshold.* Intuitively, doctors stop inquiring to inform diseases when they are *confident* that inquiring about more symptoms would not overturn his diagnosis. Therefore, we propose the decision threshold (DT) to mimic such an introspective process, that is, the agent would stop inquiring to inform the preferred disease *if the agent believes that the probability of the preferred disease is high enough so that inquiring more symptoms would not overturn the preferred disease probabilistically*. To estimate the probability of each disease and its confidence, bootstrapping technique [72, 71, 69] is adopted to train ensembles of diagnosers.

Bootstrapping diagnosers are trained to diagnose using the final state of the dialogue. The training final states are generated using the states that are sampled from the data buffer with replacement. The target of diagnoser  $i$  with parameter  $\phi_{B,i}$  is

$$\min_{\phi_{B,i}} \sum_{(\hat{\mathbf{s}}, d)} \text{CE}(f_{\phi_{B,i}}(\hat{\mathbf{s}}), d) \quad \text{s.t.} \quad \forall i \in [1, B]. \quad (4)$$

The final states generated in the intervener are then fed into  $B$  bootstrapping diagnosers, resulting in a final disease probability set  $\{\mathbf{p}_t^{(k,b)}\}_{k=1, b=1}^{K,B}$ . The final disease probability set is then used to calculate the expectation  $\boldsymbol{\mu}_t = [\mu_t^{(1)}, \dots, \mu_t^{(m)}]$  and standard deviation  $\boldsymbol{\sigma}_t = [\sigma_t^{(1)}, \dots, \sigma_t^{(m)}]$  of diseases:

$$\boldsymbol{\mu}_t = \frac{1}{KB} \sum_{b=1}^B \sum_{k=1}^K \mathbf{p}_t^{(k,b)}, \quad \boldsymbol{\sigma}_t^2 = \frac{1}{KB} \sum_{b=1}^B \sum_{k=1}^K (\mathbf{p}_t^{(k,b)} - \boldsymbol{\mu}_t)^2, \quad (5)$$

which are further used to calculate the confidence intervals of diseases. Moreover, bootstrapping diagnosers are also popular in reducing the unexpected noisy effect introduced by the data sampling process and parameters initialization. This kind of noisy effect would hamper the model's in-distributional performance [69].

With the mean and standard deviation, DT would be

met if the probability of the preferred disease is beyond the upper bound of the  $6\sigma$  confidence interval [79, 80] of the other diseases' probabilities. Denote the preferred disease as  $i$ , i.e.,  $i = \text{argmax}_j \mu_t^{(j)}, \forall j \in [1, m]$ . DT is formulated as

$$\text{DT}(\boldsymbol{\mu}_t, \boldsymbol{\sigma}_t) = \begin{cases} \text{True}, & \forall j \neq i, \mu_t^{(i)} > \mu_t^{(j)} + 3\sigma_t^{(j)}, \\ \text{False}, & \text{otherwise} \end{cases}. \quad (6)$$

**Inquiry Branch:** The diagnosis branch depends on the inquiry branch to explore the meaningful symptoms. The latter branch follows the  $Q$  network [81], which takes the concatenation of the state  $\mathbf{s}_t$  and the current disease probabilities  $\mathbf{u}_t$  to predict the action  $a_t$ .

$$a_t = \max_a Q(\mathbf{s}_t, \mathbf{u}_t, a; \theta). \quad (7)$$

The parametrized policy is trained by following the gradient:

$$\nabla_{\theta} L = \mathbb{E}_{\mathbf{s}_t, \boldsymbol{\mu}_t, a_t, \mathbf{s}_{t+1}, \boldsymbol{\mu}_{t+1}} \left[ \left( r_t + \gamma \max_a Q(\mathbf{s}_{t+1}, \mathbf{u}_{t+1}, a; \theta_{\text{targ}}) - Q(\mathbf{s}_t, \mathbf{u}_t, a_t; \theta) \right) \nabla_{\theta} Q(\mathbf{s}_t, \mathbf{u}_t, a_t; \theta) \right], \quad (8)$$

where the parameter  $\theta_{\text{targ}}$  represents the target  $Q$  network updated with the discounted factor  $\alpha$  to stabilize the training,

$$\theta_{\text{targ}} = \alpha \theta_{\text{targ}} + (1 - \alpha) \theta. \quad (9)$$

**Reward for a single goal:** Existing RL methods [4, 3] design a complex reward function to train the policy to maximize the accumulated rewards. However, the design of reward is sensitive to different scenarios, making the meaning of the accumulated rewards too complex to be understood. By disentangling the disease diagnosis from the policy, the goal of the policy becomes specific: meeting DT as soon as possible. Therefore, the reward is set as a constant  $r_t = -0.1$  to encourage the agent to meet DT rapidly.

### 3.5. Summary

Our CA-MAD framework consists of the propensity-based patient simulator and the progressive assurance agent to reduce several harmful biases. In PBPS, the propensity score estimator is learned according to Equ. (1) (propensity score learning) and the similar records are matched with similarity weight calculated in Equ. (2) (matching).

As for the diagnosis agent, the invention process is adopted to mitigate the distributional inquiry bias. Specifically, we train an intervener to infer the simulated patient from its inquired observation according to Equ. (3) (SEM (vi)). The agent diagnoses according to the inquired observation and the estimated non-inquired observation (SEM (vii)). We use bootstrapping diagnosers and different cases of estimated non-inquired observation to model the diagnostic uncertainty for our agent, formulated as Equ. (5)

(SEM (viii)). On the medical automatic diagnosis task, the uncertainty is crucial (which has also been ignored by previous methods), we believe it’s responsible to model the uncertainty to indicate whether the system works correctly.

As for the inquiry policy, different from standard RL methods, whose action is simply promoted by policy, the action in our model is regulated by the causality-aware diagnosis branch as mentioned above through the decision threshold (Equ. (6)). This regularization drives the policy to learn to capture the relation between symptom inquiry and disease diagnosis to fulfill the diagnosis requirement of the diagnosis branch.

#### 4. Experiments

To justify the effectiveness of our CA-MAD, we mainly focus on answering the following questions: **1)** *Is the propensity-based patient simulator better at answering counterfactual symptom inquiries? (Reducing default-answer bias)* **2)** *Does the progressive assurance agent achieve better in-distribution and out-of-distribution diagnostic performance? (Reducing distributional inquiry bias)* **3)** *Does the decision threshold mechanism bring about a more robust diagnosing process?*

We perform extensive and comprehensive evaluations on two MAD benchmarks, *i.e.*, MuZhi (**MZ**) [4] composed of 586 training and 142 test records with 66 symptoms and 4 diseases; DingXiang (**DX**) [3] composed of 423 training and 104 test records with 41 symptoms and 5 diseases. More details about the benchmarks are placed in Appendix C.1.  $\mathcal{P}^{\text{train}}$  and  $\mathcal{P}^{\text{all}}$  denote the patient simulators organized by the training records and all records (for training and testing) respectively. For instance,  $\mathcal{P}_{\text{PBPS}}^{\text{train}}$  represents the PBPS using training records in a benchmark to interact with the agent. Note that, all evaluation results are calculated by averaging the results from **five runs** with different random seeds. The standard deviation is provided in each table and plot (shadow areas). More numerical running examples, converging curves, hyperparameter analysis, and extended experiments are presented in Appendix D.

**Baselines.** To answer Question 1), we have compared our PBPS with PS [4, 3] and a generative world model (GEN) [13]. GEN is trained with Equ. (3) like our PBPS, while our PBPS conducts further propensity score matching to eliminate the collider biases. To our knowledge, all prior MAD works did not propose new patient simulators but used PS with the default-answer strategy. As for Question 2), we have compared our P2A against three baselines using our PBPS, *i.e.*, DQN [4], KR-DQN [3], and PG-MI-GAN [5]. DQN combines symptom inquiry and disease diagnosis into a single policy network and trains it by deep Q-learning [10, 9]. Improved from DQN, KR-DQN [3] adds a knowledge-routing module at the head of the policy using predefined disease-symptom knowledge, *i.e.*, matrices of conditional/joint probability.

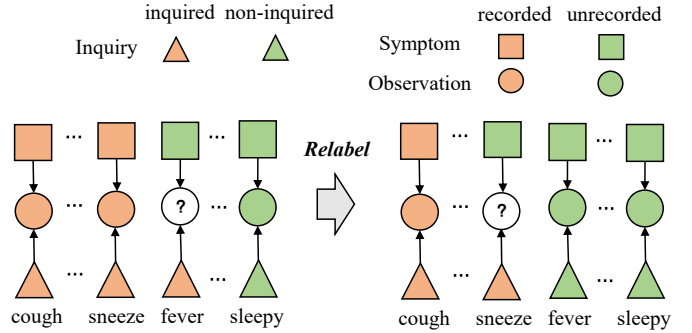


Figure 8: The sketch of the Inference Ability metric. In the original records, there is no label for the unrecorded observation (marked with ‘?’ in the left figure). The relabeling process turns the recorded symptom and observation into unrecorded (right figure). Specifically, the relabeled ‘unrecorded’ observation shares the label with the original observation.

Distinguished from DQN and KR-DQN, our P2A disentangles the disease diagnosis from the policy. Similar to ours, PG-MI-GAN [5] adopts a separate diagnoser from the inquiry policy. Specifically, it trains an inquiry generator to generate a sequence of inquiries indistinguishable by the discriminator, and further uses a pretrained diagnoser to finetune the generator. Its inquiry generator is pretrained through imitation, which lacks reasoning between inquiries and diseases. Moreover, its diagnoser is fixed during the finetuning process and does not evolve with the inquiry generator. To testify the robustness and safeness of the decision threshold mechanism (*i.e.*, Question 3), we examine whether the accuracy of P2A can be improved significantly when the decision threshold is met during diagnosing under both **In.** and **Out.** settings.

##### 4.1. Evaluation on PBPS

In the patient simulator, we are interested in whether the simulator can answer the counterfactual symptom inquiries. Therefore, we propose a novel and causal metric, namely, *Inference Ability*.

**Inferential ability.** Factually, there is no ground truth for the counterfactual symptom inquiries. In MAD, fortunately, we know what should have been observed if the inquired symptom was not inquired about, that’s, ‘not sure’, as shown in Fig. 2. This allows us to convert some recorded symptoms to be unrecorded and relabel their observation as ‘not sure’ to synthesize new records. Building simulators with the relabeled records, we can examine how the simulators answer the counterfactual symptom inquiries by inquiring about the relabeled symptom inquiries. After that, we can use the original observations to compare with the answers from the simulators. That’s the philosophy of our proposed *Inference Ability* measurement. The idea of the relabeling process of our IA metric is illustrated in Fig. 8. To measure the inferential ability (IA) of a patient simulator, we relabel all implicit symptoms from the records and only provide the explicit symptoms and

Table 1: The quantitative evaluation of the patient simulators by using the Inferential Ability (IA) metric.

Benchmarks	PS [3, 4]	GEN [13]	PBPS*	PBPS
MZ	0.0±0.0	0.12±0.01	0.57±0.02	<b>0.62±0.02</b>
DX	0.0±0.0	0.14±0.03	0.58±0.03	<b>0.66±0.01</b>

Table 2: The quantitative evaluation of the patient simulators by using the SD metric.

Benchmarks	PS [3, 4]	GEN [13]	PBPS
MZ	0.085	0.081	0.425
DX	0.116	0.110	0.438

disease to the patient simulators. After that, we inquire about the relabeled symptom of different patient simulators and calculate the accuracy of their responses. Such evaluation procedure is formulated as:

$$IA = \frac{1}{D} \sum_{p \in \text{testset}} \frac{1}{|s'|} \sum_{y_a \in s' \wedge y_a \neq 0} P(\mathcal{P}^{\text{train}}(\mathbf{s}, a; p_s) = y_a), \quad (10)$$

where  $\mathbf{s}$  represents the explicit symptoms, and  $\mathbf{s}'$  represents the implicit symptoms of the test record  $p$ , and  $p_s$  is the test record  $p$  with only its explicit symptoms observed, and  $D$  is the size of the test set, and  $|s'|$  is the number of the implicit symptoms. By this means, if a patient simulator is better at inferring non-inquired symptoms, the averaged accuracy will be higher. In our experiment, we split the complete dataset (including training samples and test samples) into five folds and calculate the cross-validation IA for each patient simulator. The results and the standard deviation are presented in Tab. 1. According to the results, the vanilla patient simulator is completely non-causal as it fails to infer any symptoms. The generative model learns the correlation without eliminating the collider biases also demonstrates a quite small IA. In contrast, our PBPS performs much better at inferring correct symptoms. We also ablate the IA of PBPS using the output of the last layer by replacing  $f_{\hat{\phi}_P}(\cdot)$  with  $f_{\phi_P}(\cdot)$  in Equ. (2), marked as PBPS\*. As shown in Tab. 1, both PBPS and PBPS\* obtain a similar IA. Since the PBPS has a more compact dimension, we conduct experiments using PBPS in the later experiments.

**Symptom density.** We also introduce an evaluation metric to quantify how informative the answers of different patient simulators are, i.e., *Symptom Density* (SD). Specifically, SD represents the proportion of informative values (-1 or 1) in the full states from the patient simulator. The higher SD means the simulator is more likely to answer an inquiry informatively. SD is calculated among  $\mathcal{P}_{\text{PS}}^{\text{train}}$ ,  $\mathcal{P}_{\text{GEN}}^{\text{train}}$ , and  $\mathcal{P}_{\text{PBPS}}^{\text{train}}$ . As shown in Tab. 2, our PBPS has obtained the highest score in SD, meaning that our PBPS can generate more informative answers. Especially, the SD of our PBPS is almost four times larger than the compared methods.

**Human evaluation.** Besides, we conduct human eval-

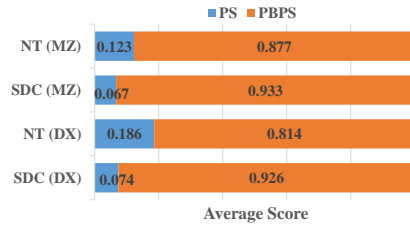


Figure 9: The comparison of human evaluation.

uation between PS and our PBPS<sup>3</sup> to distinguish which simulator is more capable of generating disease-related answers from the angle of the human doctor. We invited six human doctors to interact repeatedly with  $\mathcal{P}_{\text{PS}}^{\text{all}}$  and  $\mathcal{P}_{\text{PBPS}}^{\text{all}}$ , and score the *Naturalness* (NT, whose answers are informative like the human patient) and the *Symptom-Disease Consistency* (SDC, whose answers are more disease-related) for each simulator per evaluation episode. More details about the human evaluation are provided in Appendix C.4.1. As observed in Fig. 9, the averaging NT and SDC of our PBPS have exceeded the PS sharply, which means in the view of human experts, our PBPS can generate more informative and disease-related answers.

#### 4.2. Evaluation on P2A

As we have answered the first question, we propose empirical studies to demonstrate the superiority of our P2A to answer the other two questions. To testify the benefits of the bootstrapping technique and the intervention adopted in our diagnosis agent, we design two test settings, i.e., in-distribution diagnosis and out-of-distribution diagnosis, respectively. In the **In.** setting, the dialogue episodes used for training and testing are all generated by interacting with  $\mathcal{P}_{\text{PBPS}}^{\text{all}}$ . In the **Out.** setting, the training dialogue episodes are generated from  $\mathcal{P}_{\text{PBPS}}^{\text{train}}$ , then the trained diagnostic agents are tested by interacting with  $\mathcal{P}_{\text{PBPS}}^{\text{all}}$ . All the test-simulated patients are invisible during training.

The first setting aims to testify the basic MAD performances of the diagnostic agents since the training episodes and testing episodes are generated from the same distribution. From another aspect, the second setting is to verify the cross-distribution generalization abilities of the diagnostic agent. In this setting, we are interested how the intervention process can help improve transportability. Note that, since the decision threshold is not always met in each dialogue episode, we define a limited number of the interactions in case the agent traverses all the symptoms among these experiments to avoid degenerating the active symptom-inquiry into a form-filling manner. To demonstrate the power of the decision threshold, we also present the diagnostic performance of our P2A where DT is satisfied (P2A-DT).

<sup>3</sup>Since GEN is similar to PS quantitatively, we didn't conduct a human evaluation on GEN to reduce the complexity of the evaluation process.

Table 3: The evaluations of MAD diagnostic success rate, across different operations in **In./Out.** settings.

Data	Setting	No bootstrapping	No intervention	P2A
MZ	<b>Out.</b>	<b>0.784±0.05</b> (-0)	0.696±0.03 (-0.088)	<b>0.784±0.04</b>
	<b>In.</b>	0.834±0.03 (-0.054)	0.864±0.02 (-0.024)	<b>0.888±0.03</b>
DX	<b>Out.</b>	0.911±0.02 (-0.017)	0.840±0.03 (-0.088)	<b>0.928±0.02</b>
	<b>In.</b>	0.924±0.02 (-0.02)	0.920±0.03 (-0.024)	<b>0.944±0.02</b>

Table 4: The evaluations of MAD diagnostic success rate, across different RL baselines in **In./Out.** settings.

Data	Setting	DQN [4]	KR-DQN [3]	PG-MI-GAN [5]	P2A
MZ	<b>Out.</b>	0.697±0.031	0.653±0.016	0.721±0.025	<b>0.784±0.035</b>
	<b>In.</b>	0.845±0.026	0.755±0.016	0.741±0.017	<b>0.888±0.032</b>
DX	<b>Out.</b>	0.880±0.024	0.709±0.011	0.676±0.020	<b>0.928±0.021</b>
	<b>In.</b>	0.932±0.018	0.777±0.014	0.733±0.024	<b>0.944±0.015</b>

Table 5: The MAD diagnostic success rate under **In.** without inquiry.

MZ		DX	
No intv.	Intv.	No intv.	Intv.
0.935±0.02	<b>0.972±0.01</b>	0.971±0.02	<b>0.981±0.02</b>

### Reduction of distributional and training biases.

To testify whether the introduced operations can help diagnose as the causal diagram implies, we are interested in whether the intervention helps improve diagnostic performance under **Out.** setting and whether bootstrapping helps improve under **In.** setting. Specifically, we compare our methods with or without either bootstrapping or intervention under two different settings. The results are presented in Tab. 3, which illustrates that the averaged effects of bootstrapping are 0.037  $(=(0.888-0.834+0.944-0.924)/2)$  and 0.009  $(=(0.784-0.784+0.928-0.911)/2)$  under **In.** and **Out.** settings, respectively. In contrast, the average effects under **In.** and **Out.** settings for intervention are 0.024  $(=(0.888-0.864+0.944-0.920)/2)$  and 0.088  $(=(0.784-0.696+0.928-0.840)/2)$ . From these results, we found that the bootstrapping technique improves the agent more under in-distribution settings while the intervention improves more under the out-of-distribution settings. Besides, we noticed under **Out.** settings of MZ, the performances with and without bootstrapping are nearly the same, which indicates that improvement across distribution is mostly due to the intervention. We also found that without intervention, the performance drops at least 0.024 among all cases. This is because intervention not only reduces the distributional bias but also eliminates the indirect effect of inquired observations on the diagnosis through the non-inquired observations, contributing to a better symptom-disease relationship modeling in general. To verify that, we also evaluate the performance of the diagnoser with all symptoms inquired, under **In.** setting (in order to remove the effect of the distributional inquiry bias). Tab. 5 demonstrates that the intervention operation

not only reduces the distributional bias but also improves the diagnoser. This explains that, under **In.** setting of DX, the performance without intervention drops slightly more than the performance without bootstrapping.

**More accurate and robust diagnosis across In./Out. settings.** In Tab. 4, we compare different baselines by evaluating the mean success rate over the last 20,000 training episodes. Our P2A outperforms the other RL baselines with a clear margin in either **In.** or **Out.** setting. Ought to be regarded that, unlike P2A, all other baselines perform very sensitively when the patient simulators are different for training and testing (the **Out.** setting).

**Intervention helps diagnosis and decision threshold improves robustness.** In Tab. 6, we can observe that the performance of our P2A without intervention, i.e., P2A/-DT no intv., is severely affected, especially under **Out.** setting. The performance of P2A-DT is much better than P2A-DT no intv. implies that intervention helps the uncertainty modeling. Especially in **Out.** setting, the success rate of P2A-DT is consistently exceeding 0.9. It means that the DT can work reliably without knowing all information even to the unfamiliar patient situation, which is quite crucial for the real-world scenario.

**PBPS is beneficial to P2A with diagnosis accuracy and uncertainty modeling.** To testify whether our PBPS is beneficial to P2A from both diagnosis performance and the accuracy of uncertainty modeling, we have also evaluated P2A with PS and our PBPS under the in-distribution setting, as shown in Fig. 10. ‘PS’ denotes P2A trained with PS. ‘PS-DT’, ‘PBPS’ as well as ‘PBPS-DT’ follow the same denotation rules. From the results, we observe that without our PBPS, the performance of P2A dropped sharply. Especially, under **In.** setting, ‘PBPS-DT’ is able to achieve near-perfect results, meaning that with responses from our PBPS, the uncertainty modeling of P2A can almost capture the actual symptom-disease relation. Besides, the improvement of accuracy with ‘DT’ is much more obvious for ‘PBPS’, which implies that the agent trained with our PBPS gains a sharp improvement

Table 6: The evaluations of MAD diagnostic success rate, across different RL baselines in **In./Out.** settings.

Data	Setting	P2A no intv.	P2A-DT no intv.	P2A	P2A-DT
MZ	<b>Out.</b>	0.696±0.03	0.716±0.03	0.784±0.03	0.907±0.03
	<b>In.</b>	0.864±0.02	0.879±0.02	0.888±0.03	0.977±0.02
DX	<b>Out.</b>	0.840±0.03	0.857±0.03	0.928±0.02	0.971±0.02
	<b>In.</b>	0.920±0.03	0.933±0.03	0.944±0.02	0.982±0.01

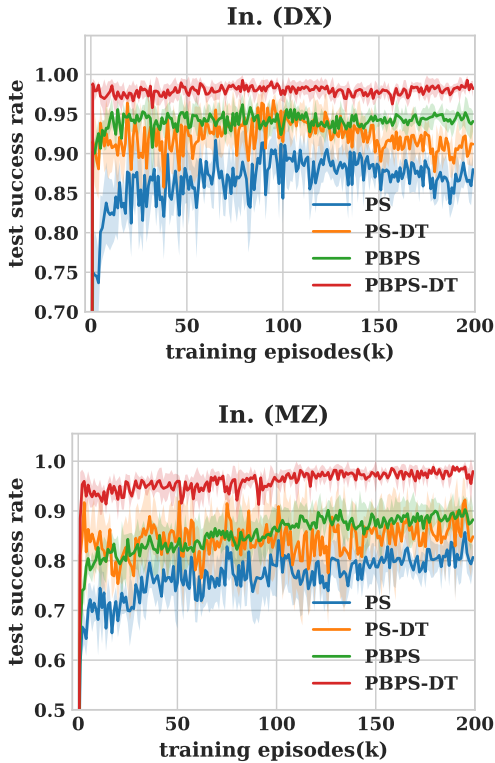


Figure 10: Performance of P2A with PS and P2A with our PBPS under **In.** setting.

performance with better uncertainty estimation.

## 5. Discussions and Limitations

In this section, we first discuss the further connection between PBPS and P2A.

### 5.1. PBPS Helps Disentangling Inquiry and Diagnosis.

Since the answers from the original patient simulator would be informative only when the inquiries are factual, state  $\mathbf{s}_t$  is prone to be insufficient to estimate the disease in the early diagnosis process. It leads the MAD agent to estimate the disease only after the symptom-inquiry process, therefore the actions of symptom inquiry and disease informing can be assigned to a single policy [4, 3]. Conversely, with our PBPS, an agent is able to gather an informative response per step. Hence, it is encouraged to learn a diagnoser to make and adjust its disease estimation along the symptom-inquiry process in parallel.

### 5.2. Better Modeling of Symptom-Disease Relationship and Diagnostic Uncertainty with Informative Causal Responses.

Since the severe sparsity of the collected record, the answers of the vanilla patient simulator are likely to be ‘not sure’, as indicated by SD in Tab. 2. Interacting with the vanilla patient simulator results in sparse and monotonous information (almost the explicit symptoms in the self-report). Sparse and monotonous information hampers the MAD agents to capture the relationship between the symptoms and diseases. The negative impact becomes even severe when the agent tries to model diagnostic uncertainty. With sparse and uninformative answers, the information during the whole diagnosis process is almost the same, therefore, the future is similar to the state of the beginning, which is not beneficial for modeling the diagnostic uncertainty. Instead, as testified in Sec. 4.2, with more informative responses from PBPS, the agent is more encouraged to model the causal relationship between symptoms and diseases as well as the uncertainty during the diagnosis to ensure robust and interpretable diagnostic results.

### 5.3. Limitations

**Enumerable inquiries and answers.** In task MAD, there are three types of answers, i.e. “Yes”, “No” and “Not sure”. And the candidate inquiries are equals to the types of symptoms. Knowing these candidate answers allows our intervener to intervene in future scenarios. However, in real-life cases, the dialogue could be more complex. Especially, the inquiries and the answers are open-vocabulary. To resolve this issue in more complex tasks, one might resort to modeling the action distribution and samples candidate actions from the distribution.

**Conservatism.** Our decision threshold imposes strict regulation on the inquiry branch. However, sometimes it could happen that the decision threshold isn’t satisfied for a long time though the intermediate diagnosis result is correct. Consequently, the dialogue became over-length. A negative example is illustrated in Appendix D. Nevertheless, for a medical application, it should be always better for the diagnostic agent to make a safer and comprehensive decision at cost of more interactions, rather than making a wrong and reckless decision. And human experts could always intervene when the diagnostic agent is hesitant to make a decision. In practice, we force the agent to stop inquiring if the length of discoursing approaches the maximum step.

## 6. Conclusion

This paper presents a complete framework for the MAD task, CA-MAD, including a simulator PBPS that tackles the problem of counterfactual symptom inquiry by PSM, and a MAD agent P2A that additionally eliminates the distributional bias via intervention and models the confidence to drive the symptom-inquiry. Through mining the passive observational data in such a collaborative representation manner, to the best of our knowledge, this paper is the first study to propose a simple yet concise paradigm to apply reinforcement learning with only passive observational data. Experimental results demonstrate that PBPS can generate more informative and disease-related answers. Moreover, P2A is more accurate and robust across distributions. Our introduced Decision Threshold provides a reliable stop mechanism for MAD agents across various settings. In the future, we will study how to extend our framework to broader ranges of sequential discriminative decision-making problems with passive observational data.

## References

- [1] S. R. Cole, R. W. Platt, E. F. Schisterman, H. Chu, D. Westreich, D. Richardson, C. Poole, Illustrating bias due to conditioning on a collider, *IJE* 39 (2) (2010) 417–420.
- [2] K.-F. Tang, H.-C. Kao, C.-N. Chou, E. Y. Chang, Inquire and diagnose: Neural symptom checking ensemble using deep reinforcement learning, in: *NeurIPS*, 2016.
- [3] L. Xu, Q. Zhou, K. Gong, X. Liang, J. Tang, L. Lin, End-to-end knowledge-routed relational dialogue system for automatic diagnosis, in: *AAAI*, 2019.
- [4] Z. Wei, Q. Liu, B. Peng, H. Tou, T. Chen, X. Huang, K.-F. Wong, X. Dai, Task-oriented dialogue system for automatic diagnosis, in: *ACL*, Vol. 2, 2018, pp. 201–207.
- [5] Y. Xia, J. Zhou, Z. Shi, C. Lu, H. Huang, Generative adversarial regularized mutual information policy gradient framework for automatic diagnosis, in: *AAAI*, 2020, pp. 1062–1069.
- [6] Z. Lipton, X. Li, J. Gao, L. Li, F. Ahmed, L. Deng, Bbq-networks: Efficient exploration in deep reinforcement learning for task-oriented dialogue systems, in: *AAAI*, 2018.
- [7] T. Wen, D. Vandyke, N. Mrkšić, M. Gašić, L. Rojas-Barahona, P. Su, S. Ultes, S. Young, A network-based end-to-end trainable task-oriented dialogue system, in: *ACL*, 2017.
- [8] Z. Yan, N. Duan, P. Chen, M. Zhou, J. Zhou, Z. Li, Building task-oriented dialogue systems for online shopping, in: *AI*, 2017.
- [9] V. Mnih, K. Kavukcuoglu, D. Silver, A. Graves, I. Antonoglou, D. Wierstra, M. Riedmiller, Playing atari with deep reinforcement learning, in: *CS*, 2013.
- [10] V. Mnih, K. Kavukcuoglu, D. Silver, A. A. Rusu, J. Veness, M. G. Bellemare, A. Graves, M. Riedmiller, A. K. Fidjeland, G. Ostrovski, et al., Human-level control through deep reinforcement learning, *Nature* 518 (7540) (2015) 529.
- [11] D. Silver, J. Schrittwieser, K. Simonyan, I. Antonoglou, A. Huang, A. Guez, T. Hubert, L. Baker, M. Lai, A. Bolton, Y. Chen, T. Lillicrap, F. Hui, L. Sifre, v. d. G. Driessche, T. Graepel, D. Hassabis, Mastering the game of go without human knowledge, *Nature* (2017) 354–359.
- [12] D. Silver, A. Huang, C. J. Maddison, A. Guez, L. Sifre, G. Van Den Driessche, J. Schrittwieser, I. Antonoglou, V. Panneershelvam, M. Lanctot, et al., Mastering the game of go with deep neural networks and tree search, *nature* 529 (7587) (2016) 484–489.
- [13] B. Peng, X. Li, J. Gao, J. Liu, K.-F. Wong, Integrating planning for task-completion dialogue policy learning, in: *ACL*, 2018.
- [14] H. Chen, X. Liu, D. Yin, J. Tang, A survey on dialogue systems: Recent advances and new frontiers, in: *SIGKDD*, ACM, 2017.
- [15] H. Bang, J. M. Robins, Doubly robust estimation in missing data and causal inference models, *Biometrics* 61 (4) (2005) 962–973.
- [16] D. B. Rubin, Estimating causal effects of treatments in randomized and nonrandomized studies., *JEP* 66 (5) (1974) 688.
- [17] J. Neyman, Sur les applications de la théorie des probabilités aux expériences agricoles: Essai des principes, *Roczniki Nauk Rolniczych* 10 (1923) 1–51.
- [18] R. H. Dehejia, S. Wahba, Propensity score-matching methods for nonexperimental causal studies, in: *RES*, Vol. 84, MIT Press, 2002.
- [19] P. C. Austin, An introduction to propensity score methods for reducing the effects of confounding in observational studies, *MBR* 46 (3) (2011) 399–424.
- [20] P. R. Rosenbaum, D. B. Rubin, The central role of the propensity score in observational studies for causal effects, in: *Biometrika*, Oxford University Press, 1983.
- [21] R. Ratcliff, P. L. Smith, S. D. Brown, G. McKoon, Diffusion decision model: Current issues and history, *Trends in cognitive sciences* 20 (4) (2016) 260–281.
- [22] S. Mithen, J. Morton, The prehistory of the mind, Thames & Hudson London, 1996.
- [23] Y. N. Harari, *Sapiens: A brief history of humankind*, Random House, 2014.
- [24] J. Pearl, Theoretical impediments to machine learning with seven sparks from the causal revolution, in: *ICWSDM*, 2018.
- [25] M. A. Hernán, J. Hsu, B. Healy, A second chance to get causal inference right: a classification of data science tasks, *Chance* 32 (1) (2019) 42–49.
- [26] J. S. B. Evans, Dual-processing accounts of reasoning, judgment, and social cognition, *ARP* 59 (2008) 255–278.
- [27] R. Sun, Duality of the mind: A bottom-up approach toward cognition, Psychology Press, 2001.
- [28] J. W. Kable, P. W. Glimcher, An “as soon as possible” effect in human intertemporal decision making: behavioral evidence and neural mechanisms, *JN* 103 (5) (2010) 2513–2531.
- [29] Y.-S. Peng, K.-F. Tang, H.-T. Lin, E. Chang, Refuel: Exploring sparse features in deep reinforcement learning for fast disease diagnosis, in: *NeurIPS*, 2018, pp. 7333–7342.
- [30] J. Pearl, et al., Causal inference in statistics: An overview, *Statistics surveys* 3 (2009) 96–146.
- [31] K. A. Bollen, J. Pearl, Eight myths about causality and structural equation models, in: *Handbook of causal analysis for social research*, Springer, 2013, pp. 301–328.
- [32] L. Chen, H. Zhang, J. Xiao, X. He, S. Pu, S.-F. Chang, Counterfactual critic multi-agent training for scene graph generation, in: *CVPR*, 2019, pp. 4613–4623.
- [33] T. Kaihua, N. Yulei, H. Jianqiang, S. Jiabin, Z. Hanwang, Unbiased scene graph generation from biased training, in: *CVPR*, 2020.
- [34] J. Qi, Y. Niu, J. Huang, H. Zhang, Two causal principles for improving visual dialog, in: *CVPR*, 2020, pp. 10860–10869.
- [35] T. Wang, J. Huang, H. Zhang, Q. Sun, Visual commonsense r-cnn, in: *CVPR*, 2020, pp. 10760–10770.
- [36] E. Abbasnejad, D. Teney, A. Parvaneh, J. Shi, A. v. d. Hengel, Counterfactual vision and language learning, in: *CVPR*, 2020.
- [37] I. Dasgupta, X. J. Wang, S. Chiappa, J. Mitrovic, A. P. Ortega, D. Raposo, E. Hughes, P. Battaglia, M. Botvinick, Z. Kurth-Nelson, Causal reasoning from meta-reinforcement learning, in: *ICLR*, 2019.
- [38] M. Oberst, D. Sontag, Counterfactual off-policy evaluation with gumbel-max structural causal models, in: *ICML*, 2019.
- [39] N. J. Foerster, G. Farquhar, T. Afouras, N. Nardelli, S. Whiteson, Counterfactual multi-agent policy gradients, in: *NCAI*, 2018.
- [40] J. Pearl, D. Mackenzie, *The book of why: the new science of cause and effect*, Basic Books, 2018.
- [41] E. Bareinboim, J. Pearl, Causal inference and the data-fusion problem, in: *Proceedings of the National Academy of Sciences*,

- Vol. 113, National Academy Sciences, 2016, pp. 7345–7352.
- [42] J. Pearl, *Causality*, Cambridge university press, 2009.
- [43] J. D. Angrist, G. W. Imbens, Two-stage least squares estimation of average causal effects in models with variable treatment intensity, in: *JASA*, Taylor & Francis Group, 1995.
- [44] R. A. Johnson, I. Miller, J. E. Freund, *Probability and statistics for engineers*, Vol. 2000, Pearson Education London, 2000.
- [45] E. A. Stuart, Matching methods for causal inference: A review and a look forward, *SS 25 (1)* (2010) 1.
- [46] J. Schatzmann, B. Thomson, K. Weilhammer, H. Ye, S. Young, Agenda-based user simulation for bootstrapping a pomdp dialogue system, in: *ACL, ACL*, 2007, pp. 149–152.
- [47] X. Li, Z. Lipton, B. Dhingra, L. Li, J. Gao, Y.-N. Chen, A user simulator for task-completion dialogues, in: *arXiv:1612.05688*, 2016.
- [48] B. Dhingra, L. Li, X. Li, J. Gao, Y.-N. Chen, F. Ahmed, L. Deng, End-to-end reinforcement learning of dialogue agents for information access, in: *ACL*, 2016.
- [49] X. Li, Y.-N. Chen, L. Li, J. Gao, A. Celikyilmaz, End-to-end task-completion neural dialogue systems, in: *IJCNLP*, Vol. 1, 2017.
- [50] A. Madotto, C.-S. Wu, P. Fung, Mem2seq: Effectively incorporating knowledge bases into end-to-end task-oriented dialog systems., in: *ACL*, 2018, pp. 1468–1478.
- [51] C.-S. Wu, R. Socher, C. Xiong, Global-to-local memory pointer networks for task-oriented dialogue, in: *ICLR*, 2019.
- [52] W. Lei, X. Jin, M.-Y. Kan, Z. Ren, X. He, D. Yin, Sequicity: Simplifying task-oriented dialogue systems with single sequence-to-sequence architectures, in: *ACL*, Vol. 1, 2018, pp. 1437–1447.
- [53] H.-C. Kao, K.-F. Tang, E. Y. Chang, Context-aware symptom checking for disease diagnosis using hierarchical reinforcement learning, in: *AI*, 2018.
- [54] M. Hutson, Ai protein-folding algorithms solve structures faster than ever, in: *Nature*, 2019.
- [55] S. R. Sutton, A. D. Mcallester, P. S. Singh, Y. Mansour, Policy gradient methods for reinforcement learning with function approximation, in: *NeurIPS*, 1999, pp. 1057–1063.
- [56] A. Rangel, C. Camerer, P. R. Montague, A framework for studying the neurobiology of value-based decision making, *Nature reviews neuroscience* 9 (7) (2008) 545–556.
- [57] J. Zhang, The effects of evidence bounds on decision-making: theoretical and empirical developments, *Frontiers in psychology* 3 (2012) 263.
- [58] L. Schmidt, A. Tusche, N. Manoharan, C. Hutcherson, T. Hare, H. Plassmann, Neuroanatomy of the vmPFC and dlPFC predicts individual differences in cognitive regulation during dietary self-control across regulation strategies, *Journal of Neuroscience* 38 (25) (2018) 5799–5806.
- [59] B. Gawronski, L. A. Creighton, *Dual process theories.*, Oxford University Press, 2013.
- [60] D. Kahneman, A perspective on judgment and choice: mapping bounded rationality., *The American psychologist* 58 9 (2003) 697–720.
- [61] G. F. Loewenstein, E. U. Weber, C. K. Hsee, N. Welch, Risk as feelings., *Psychological bulletin* 127 (2) (2001) 267.
- [62] L. Buchen, Neuroscience: Illuminating the brain, *Nature* 465 (2010) 26–8. doi:10.1038/465026a.
- [63] R. Ratcliff, G. McKoon, The Diffusion Decision Model: Theory and Data for Two-Choice Decision Tasks, *Neural Computation* 20 (4) (2008) 873–922. doi:10.1162/neco.2008.12-06-420.
- [64] T. J. VanderWeele, A three-way decomposition of a total effect into direct, indirect, and interactive effects, *Epidemiology (Cambridge, Mass.)* 24 (2) (2013) 224.
- [65] J. Pearl, Causal diagrams for empirical research. *biometrika*, in: *MathSciNet*, Vol. 860, 1995.
- [66] D. Koller, N. Friedman, *Probabilistic graphical models: principles and techniques*, MIT press, 2009.
- [67] Y. Huang, M. Valtorta, Pearl’s calculus of intervention is complete, in: *CUAI*, 2012.
- [68] I. Shpitser, J. Pearl, Identification of conditional interventional distributions, in: *CUAI*, 2012.
- [69] R. McAllister, G. Kahn, J. Clune, S. Levine, Robustness to out-of-distribution inputs via task-aware generative uncertainty, in: *ICRA*, 2019.
- [70] J. Pearl, E. Bareinboim, External validity: From do-calculus to transportability across populations, *Statistical Science* (2014) 579–595.
- [71] P. Whaite, F. P. Ferrie, Autonomous exploration: Driven by uncertainty, *TPAMI* 19 (3) (1997) 193–205.
- [72] P. Whaite, F. P. Ferrie, From uncertainty to visual exploration, *TPAMI* 13 (10) (1991) 1038–1049.
- [73] I. Osband, J. Aslanides, A. Cassirer, Randomized prior functions for deep reinforcement learning, in: *NeurIPS*, 2018.
- [74] Y. Burda, H. Edwards, A. Storkey, O. Klimov, Exploration by random network distillation, in: *ICLR*, 2019.
- [75] E. Todorov, T. Erez, Y. Tassa, Mujoco: A physics engine for model-based control, in: *IROS, IEEE*, 2012.
- [76] J. Pearl, The do-calculus revisited, in: *UAI*, 2012.
- [77] M. A. Hernan, J. Robins, *Causal inference* (2019).
- [78] C. M. Bishop, *Pattern recognition and machine learning*, springer, 2006.
- [79] P. S. Pande, L. Holpp, *What is six sigma?*, McGraw-Hill Professional, 2001.
- [80] E. Parzen, *Modern probability theory and its applications*, John Wiley & Sons, Incorporated, 1960.
- [81] Z. Wang, T. Schaul, M. Hessel, H. Van Hasselt, M. Lanctot, N. De Freitas, Dueling network architectures for deep reinforcement learning, in: *ICML*, 2016.
- [82] S. L. Morgan, C. Winship, *Counterfactuals and causal inference*, Cambridge University Press, 2015.

## Appendix A. Propensity-based Patient simulator (PBPS)

### Appendix A.1. Propensity Score Matching (PSM)

In real life, we can only observe the outcome of the actual action, which is named as the factual outcome. However, sometimes we might wonder what the outcome should have been if the other action had been taken, that is the counterfactual outcome. The potential outcome can be either factual or counterfactual. According to the potential outcome framework [16, 17], the counterfactual outcome is inferable if the three assumptions are met: the stable unit treatment value assumption (SUTVA), consistency and ignorability (unconfoundedness). Ordinarily, SUTVA and consistency are assumed to be satisfied. With ignorability, we assume that all the confounding variables are observed and reliably measured by a set of features  $X^{(u)}$  for each instance  $u$ .  $X^{(u)}$  denotes a set of confounding variables, namely a subset of features that describes the instance  $u$  and causally influences the values of both the treatment  $A^{(u)}$  and the potential outcome  $Y_a^{(u)}$ . Ignorability means that the values of the potential outcomes  $Y_a^{(u)}$  are independent of the factual action  $A^{(u)}$ , given  $X^{(u)}$ . Mathematically, ignorability can be formulated as:

$$Y_a^{(u)} \perp\!\!\!\perp A^{(u)} | X^{(u)}. \quad (\text{A.1})$$

From the notation, we can see that this is an assumption defined at the individual level. With ignorability satisfied, we can estimate the counterfactual outcome of  $u$  through the factual outcomes of other instance  $u'$  with the same covariates  $Y_a^{(u)} = Y_a^{(u')} | X^{(u)} = X^{(u')}$ , which is the essence of *the matching methods* [45].

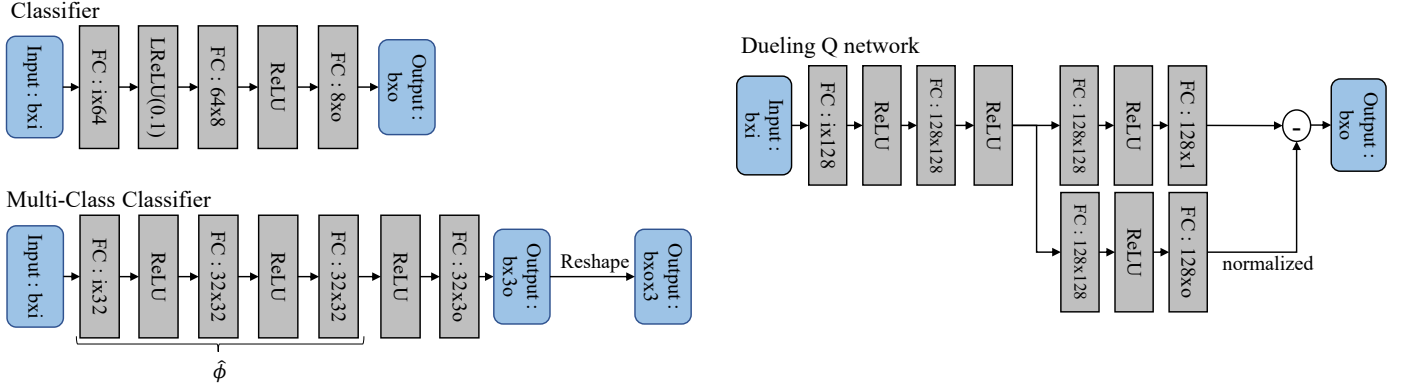


Figure 11: Two types of network structures used throughout the whole work, i.e. "Classifier" (upper) and "Multi-Class Classifier" (lower). "FC" is the abbreviated form of a fully connected layer, and "LReLU(0.1)" is the abbreviated form of leaky ReLU activation with a negative slope as 0.1.  $b$  denotes the batch size of the input and  $i$  denotes the input dimension.

However, we need to be careful when there exists a group which only contains instances with only one type of action. We cannot estimate the counterfactual outcome in this group. This issue is referred to as *the lack of overlap*. To overcome this issue, the most widely adopted matching as weighting methods specify the function  $e(X^{(u)})$  in estimating *propensity score*  $P(A^{(u)}|X^{(u)})$  [82]. We need to make sure whether the ignorability still holds with  $e(X^{(u)})$ . In other words, given  $e(X^{(u)})$ , whether the  $Y_a^{(u)} \perp\!\!\!\perp A^{(u)} | e(X^{(u)})$  still holds. We show that  $Y_a^{(u)} \perp\!\!\!\perp A^{(u)} | e(X^{(u)})$  is satisfied in the following. Here, for briefness,  $(Y, X, A)$  denotes  $(Y_a^{(u)}, X^{(u)}, A^{(u)})$ .

$$\begin{aligned} P(A|e(X)) &= \mathbb{E}[A|e(X)] = \mathbb{E}[\mathbb{E}[A|X, e(X)]|X] \\ &= \mathbb{E}[\mathbb{E}[A|X]|X] = \mathbb{E}[e(X)|X] = e(X) \end{aligned} \quad (\text{A.2})$$

$$\begin{aligned} P(Y, A|e(X)) &= P(Y|e(X))P(A|Y, e(X)) \\ &= P(Y|e(X))\mathbb{E}[P(A|Y, e(X), X)|X] \\ &= P(Y|e(X))\mathbb{E}[P(A|Y, X)|X] \\ &= P(Y|e(X))\mathbb{E}[P(A|X)|X] \quad \text{by ignorability} \\ &= P(Y|e(X))\mathbb{E}[e(X)|X] \\ &= P(Y|e(X))e(X) \\ &= P(Y|e(X))P(A|e(X)) \quad \text{according to (A.2)} \end{aligned} \quad (\text{A.3})$$

From (A.3), we know that  $Y_a^{(u)} \perp\!\!\!\perp A^{(u)} | e(X^{(u)})$ . It means that we can estimate the counterfactual outcome of  $u$  by matching instances with the same propensity score  $e(X^{(u)})$ .

#### Appendix A.2. Details of PBPS

To show that PSM is workable in our patient simulator, we need to show the ignorability is satisfied given the covariates  $X^{(p)} = (\mathbf{y}^{(p)}, d^{(p)})$  of the record  $p$ , i.e.,  $Y_a^{(p)} \perp\!\!\!\perp A^{(p)} | (\mathbf{y}^{(p)}, d^{(p)})$ , where  $Y_a^{(p)}$  and  $A^{(p)}$  is the random variables for the potential existence of symptom and the factual symptom inquiry,  $\mathbf{y}^{(p)}$  is the observed symptoms

and  $d^{(p)}$  is the ground-truth disease of the record  $p$ . A reasonable assumption is that the symptom inquiry  $A^{(p)}$  is only dependent on the history observed symptoms  $\mathbf{y}^{(p)}$ , and the existence of symptom  $Y^{(p)}$  is only dependent on the disease  $d^{(p)}$ . Here, for briefness,  $(Y, A, \mathbf{y}, d)$  denotes  $(Y_a^{(p)}, A^{(p)}, \mathbf{y}^{(p)}, d^{(p)})$ . Then we have

$$P(Y, A|\mathbf{y}, d) = P(Y|d)P(A|\mathbf{y}) = P(Y|\mathbf{y}, d)P(A|\mathbf{y}, d). \quad (\text{A.4})$$

From (A.4), we know that the ignorability  $Y_a^{(p)} \perp\!\!\!\perp A^{(p)} | (\mathbf{y}^{(p)}, d^{(p)})$  holds. According to the PSM, the propensity score in MAD could be  $e(\mathbf{y}^{(p)}, d^{(p)}) = P(A^{(p)}|\mathbf{y}^{(p)}, d^{(p)})$ . Nevertheless, we not only want the probability of symptom inquiry to be matched but also the symptom existence to be matched. To this, we adopt a more strict propensity score

$$\begin{aligned} P(Y_a|\mathbf{y}, d) &= P(A, Y_A|\mathbf{y}, d) = P(A|\mathbf{y}, d)P(Y_A|A, d) \\ &= e(\mathbf{y}, d)P(Y_A|A, d). \end{aligned} \quad (\text{A.5})$$

Again,  $Y_a^{(p)} \perp\!\!\!\perp A^{(p)} | P(Y_a|\mathbf{y}, d)$  is satisfied because matching  $P(Y_a|\mathbf{y}, d)$  implies matching  $e(\mathbf{y}^{(p)}, d^{(p)})$ . Assuming the symptom existence is only dependent on the disease  $d$  and the observed symptoms, then the propensity score for all symptoms is  $f(\mathbf{y}, d) = P(\mathbf{Y}|\mathbf{y}, d)$

The multi-classifier adopted for training the propensity score  $f_{\phi_P}(\mathbf{y}, d)$  with parameter  $\phi_P$  is shown in Fig. 11, whose intermediate result  $f_{\phi_P}(\mathbf{y}, d)$  from the second to the last FC layer is used as the patient propensity score as it's more compact. The input dimension  $i$  is set as  $m + n$  and the output dimension  $o$  is set as  $n$ , where  $m$  is the number of diseases, and  $n$  is the number of symptoms. During training, the input is masked with an random binary mask  $\mathbf{m}$  resulting in  $(\mathbf{y} \odot \mathbf{m}, d)$ , and the target is to recover the original information  $\mathbf{y}$ . Given the anchor record  $p$ , we first calculate the propensity scores of the other records  $q$ . Since for the anchor  $p$ , the observed covariates information is  $(\mathbf{y}^{(p)}, d^{(p)})$ . Therefore, we only match the anchor record with the others ignoring the unobserved symptoms. Thus,

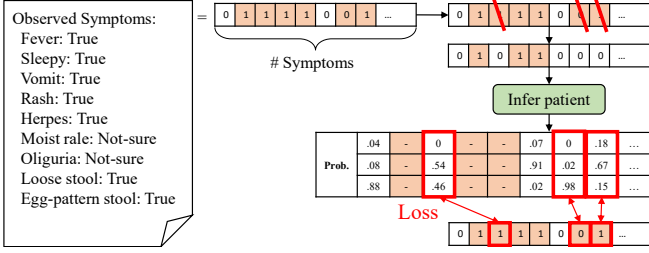


Figure B.12: Training strategy of the intervener. The inquired information is masked off and the intervener is trained to recover them back.

the propensity of  $q$  according to  $p$  is  $f_{\hat{\phi}_P}(\mathbf{y}^{(q)} \odot \mathbf{m}^{(p)}, d^{(q)})$ , where  $\mathbf{m}^{(p)} = [\mathbb{I}(y_a \neq 0), \forall a \in [1, \dots, n]]$ . The similarity weight  $P(q|p, a)$  is then calculated according to  $f_{\hat{\phi}_P}(\mathbf{y}^{(p)}, d^{(p)})$  and  $f_{\hat{\phi}_P}(\mathbf{y}^{(q)} \odot \mathbf{m}^{(p)}, d^{(q)})$ .

## Appendix B. Progressive Assurance Agent (P2A)

### Appendix B.1. Details of P2A

#### Appendix B.1.1. Intervener

Similar to the PBPS, we adopt the multi-classifier network in Fig. 11 for the intervener. This intervener is aimed at predicting the final state  $\hat{\mathbf{s}}_t$  according to the current visited symptoms  $\mathbf{s}_t^v$ . Therefore, we model it as a generative problem.  $\phi_G$  is the parameter of the generator  $f_{\phi_G}(\cdot)$ . The input dimension  $i$  and the output dimension  $o$  are both set as  $n$ .  $N$  is the number of final states in the buffer. The Monte Carlo sampling is applied according to the generative model  $f_{\phi_G}(\mathbf{s}_t)$  to sample a set of possible final states  $\{\hat{\mathbf{s}}\}$ . Note that, the visited symptoms of  $\mathbf{s}_t^v$  remain the same in the generated final states  $\{\hat{\mathbf{s}}\}$ .

#### Appendix B.1.2. Bootstrapping diagnosers

The network structure of the bootstrapping diagnoser is the classifier structure in Fig. 11. The input dimension is set as  $n$ , and the output dimension is set as  $m$ . The input  $\hat{\mathbf{s}}_t$  is sampled from the intervener, and the target  $d$  is collected at the end of the episodes. During training, the training data are sampled with replacement from the data buffer, in order to eliminate the sampling bias caused by the training data sampling and focus on estimating the uncertainty of the network parameters. At the end of each diagnosis, the final observed state and the ground-truth disease are stored in a data buffer. To train the intervention module, we sample states from that buffer, and mask off several observed symptoms and use the new state as the input. We only calculate the cross-entropy loss for the masked symptoms since we only have labels for these symptoms. An intuitive demonstration of the training process is as Fig. B.12. As for training the diagnoser, we also sample states from that data buffer and forward these states to the intervention module to generate full states as input to the diagnoser.

### Appendix B.1.3. Policy network

The Q-learning policy network we adopted is the Dueling-DQN [81] in Fig. 11 for stabilizing the training procedure, which has two heads with one for state value  $V$  and the other one for action advantage value  $A$ . Therefore,  $Q(\mathbf{s}_t, \boldsymbol{\mu}_t, a_t) = V(\mathbf{s}_t, \boldsymbol{\mu}_t) + A(\mathbf{s}_t, \boldsymbol{\mu}_t, a_t)$ , where  $\boldsymbol{\mu}_t$  is the expectation of disease probability calculated from the output of the bootstrapping diagnosers. In order to avoid repeating choosing symptoms have been visited, we subtract 1000000 for each symptom has been inquired from the  $Q(\mathbf{s}_t, \boldsymbol{\mu}_t, a_t)$  to decrease the q values of these symptoms. The input contains three vector, i.e., the state  $\mathbf{s}_t$ , the inquired history  $[\mathbb{I}(s_{t,a} \neq -2), \forall a \in [1, \dots, n]]$  and the expectation of diseases' probabilities  $\boldsymbol{\mu}$ . Therefore, the input dimension  $i$  is set as  $2 \times n + m$  and the output dimension  $o$  is set as  $n$ .

## Appendix C. Experiment Details

### Appendix C.1. Benchmark Examples

In this part, we briefly describe the data format of two open benchmarks, MZ (MuZhi) [4] and DX (DingXiang) [3]. The diagnosis record from MZ is clean and structural in which original dialogue sentences are not preserved. Different from MZ and DX that preserve the original sentences of the self-report. In both datasets, the record contains the ground-truth disease "disease\_tag", the symptom information extracted from the original self-report "explicit\_inform\_slots", and also the symptom information mentioned during the original dialogue "implicit\_inform\_slots". Two examples from these datasets are demonstrated in Fig. C.13. Notice that, these two datasets are in Chinese originally and we translate them into English to demonstrate in this paper.

### Appendix C.2. Training Details

For training the propensity score estimator of PBPS, the learning rate is 0.01 initially and is decreased to the tenth of it for every 10000 iterations. The total training iterations is 40000 with the Adam optimizer. The batch size  $b$  is 128.

For training the P2A, the learning rate of the policy network is 0.001 and is decreased to the tenth of it after 100,000 training episodes while the learning rate for the intervener and the bootstrapping diagnosers is fixed at 0.001. All of the parameters are updated by the Adam optimizer. The maximum number of training episodes is 200,000. The max dialogue rounds  $T$  is  $1/3 \times N$ . The constant reward -0.1 is given to the agent for each round to encourage the shorter dialogues. The  $\epsilon$  of  $\epsilon$ -greedy strategy is set to 0.1 for efficient action space exploration, and the discount factor  $\gamma$  in the Bellman equation is 0.95. The size of buffer  $\mathcal{D}_Q$  is 50,000 and the size of buffer  $\mathcal{D}_C$  is 1280. The batch size is 32, and the Polyak factor is 0.99. The number of samples of the intervener is set as 50, and the number of the bootstrapping models is 10. We update

Record from MuZhi:

```
{
  'disease_tag':
    '小儿消化不良' ('infantile diarrhea'),
  'implicit_inform_slots': {
    '便秘' ('constipation'): True,
    '屁' ('fart'): True
  },
  'explicit_inform_slots': {
    '消化不良' ('indigestion'): True,
    '稀便' ('loose stool'): True
  }
}
```

Record from DingXiang:

```
{
  'disease_tag':
    '小儿手足口病' ('infantile hand foot mouth disease'),
  'explicit_inform_slots': {
    '疱疹' ('herpes'): True,
    '咳嗽' ('coughing'): True,
    '烦躁不安' ('fidgety'): True
  },
  'implicit_inform_slots': {
    '发烧' ('fever'): False
  },
  'self_report': '十个月宝宝，嘴里突然长了很多白色的泡
    泡，请问是什么东西？最近有点咳嗽。天有点热，长了很
    多痱子，喜欢用手去挠。昨天晚上有点闹。今天早上也是'
    ('Ten months baby's mouth grows a lot of white herpes. What
    happened to him? He has been coughing a little recently. He
    grows a lot of heat rash and cannot help scratching with hands.
    He was a bit fidgety last night and this morning.')
}
```

Figure C.13: The record examples from benchmarks MuZhi (MZ) [4] and DingXiang (DX) [3]. The upper record is sampled from MZ, which is in a structural and clean format. The bottom record is sampled from DX, different from MZ, whose original self-report is preserved. Both benchmarks are in Chinese and we present them in English in this paper.

the target policy every ten rounds and update the model every round after 6,000 random start rounds.

### Appendix C.3. Baselines details

The RL baselines DQN [4] and KR-DQN [3] are trained with the open-source code from KR-DQN [3] with default training settings. Moreover, the batch size for training is set as 32, and the learning rate is 0.001, which will decrease to the tenth of it after every 40000 iterations with the Adam optimizer. The total training iterations is set as 100000.

### Appendix C.4. Evaluation for Patient Simulator

#### Appendix C.4.1. Human evaluation details

In order to measure the qualitative performance of the patient simulators, i.e. PS and PBPS, we propose ‘Naturalness’ (NT) and ‘Symptom-Disease Consistency’ (SDC) metrics. NT is to score how natural the simulator is (we ask the human experts: “Which one is more natural?”)

and SDC is to score whether the patient simulator can generate disease-related responses (we ask the human experts: “Which one is more disease-related?”). The reason that we use NT instead of informativity (corresponding to ‘informative’) is that informativity can be well quantified by the ‘Symptom Density’ proposed in the quantitative evaluation. Realizing that the ultimate goal of the quantitative and qualitative evaluations is to find out which patient simulator is more like a human patient, we decide to employ the more essential yet more subjective index, i.e., ‘Naturalness’.

The experts were required to decide which simulator is more natural (score 1) and which simulator is more disease-related (score 1) per episode with the two patient simulators. We invited six human doctors and made each doctor interact with the two patient simulators with 30 episodes (5 interactions each episode) with random anchor records from each dataset. We adopted the simple template-based natural language generator for both the patient simulators to respond to the doctor’s inquiry simultaneously. As for the doctors, we offered them the list of symptoms of each dataset. For each evaluation episode, one random anchor record was chosen for both the patient simulators, and the doctors were provided with the self-report and the corresponding ground truth disease of the anchor record. Then the doctor would initiate the inquiries about symptoms which would be answered by both patient simulators without knowing which answer is from which patient simulator. After interviewing, we counted the proportion of NT and SDC for each patient simulator by dividing the total number of samples, i.e.  $6 \times 30$  (6 doctors and 30 samples for each dataset and each patient simulator).

In order to provide more comprehensive statistical results of the human evaluation, we also provided the mean and standard deviation of scores from different human participants in Tab. C.7 and the P-value [44] of each human evaluation result as shown in Tab. C.8. 1 denotes our approach better, 0 otherwise. In Tab. C.7, a value greater than 0.5 means our simulator is better (0.5 means tie statistically). As can be seen from the table, for each participant and each measurement, our proposed method always scores higher statistically. Notice that since the score is a binary value from 0, 1, the standard deviation becomes larger when the expectation approaches 0.5. In Tab. C.8, the null hypothesis of each index is that two patients are assumed to be even, and the expectation value is 0.5. The p-value is one-tailed since we only need to consider how significant the claim that our method is better than the original. The significance level is set as 0.05 empirically [44]. From the results in the table, we can observe that all p-values are pretty small, which means our claims are always significant across different benchmarks and measures.

#### Appendix C.5. More Experimental Results

**Performance improvement of MAD agents.** As the answers from PBPS are more realistic, we have veri-

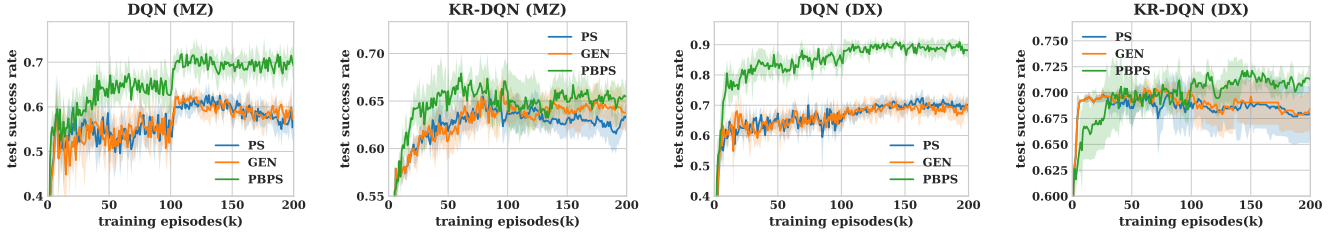


Figure C.14: The success-rate curves of the original patient simulator (PS) [3, 4], generative world model (GEN) [13], and our probabilistic-symptom patient simulator (PBPS) based on DQN [4] and KR-DQN [3] trained in the benchmarks MZ and DX, respectively.

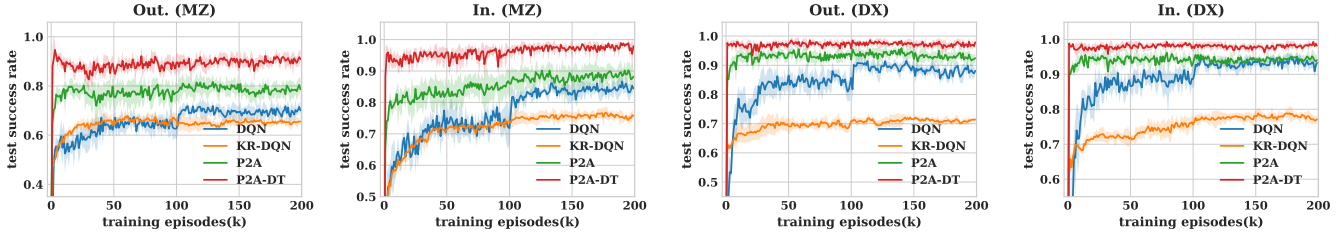


Figure C.15: The comparison of DQN [4], KR-DQN [3], and P2A on MZ and DX across In./Out. evaluation settings. The curves denote the mean of the success rate over iterations with deviations.

fied whether PBPS can be more beneficial to existing RL baselines than the original simulator. In specific, we take  $\mathcal{P}^{\text{train}}$  to interact with the DQN and KR-DQN agents to train their policies, then, we evaluate their success rates on the diagnosis episodes generated by completing the absent value of the symptoms in the test set of the MAD benchmarks. Fig. C.14 showcases the comparisons between the PS and PBPS based on success rates across RL baselines and benchmarks. We have observed that when trained with the episodes generated by PBPS, the RL baselines reap a significant performance over the original. It evidences that using PBPS helps to develop more competitive MAD agents for real-world applications.

**Fast convergence and abrupt availability of diagnostic knowledge.** In dual-process theory, the learning of the top-level process is often rule-regulated and represents the abrupt availability of explicit knowledge. Similar to our P2A, the diagnosis branch acts as the top-level process and learns how to diagnose regulated by the non-parametric decision threshold. According to the experimental results in Fig.C.15, we have also observed the abrupt availability of the diagnosis when the decision threshold is satisfied. Fig.C.15 illustrates the success rate over the iteration of the training episodes required to train the RL agents. P2As (P2A and P2A-DT) achieve faster convergence and higher success rates in upper bounds than all other baselines. Remarkably, those episodes that met the DT achieve a very high success rate even at the very beginning of the training phase (red curve), meaning that DT only needs a small amount of training data to work reliably (i.e., the abrupt availability of diagnostic knowledge). Such reliable diagnosing performance is significant specifically in the MAD task as the data are expensive to collect.

**Selection of hyperparameters.** In this part, we conduct extra ablation studies of our proposed method to

understand the sensitivity of different hyperparameters. Especially, despite those basic hyperparameters such as learning rate and decay frequency that are used in all baselines, there are several important hyperparameters that are special in our methods. They are discount factor  $\gamma$  adopted in Bellman backup, the number of bootstrapping diagnosers for estimate uncertainty, the generative sample number of the intervener, and the reward signal designed to drive the learning process. For the exposition, we evaluate our method on the MZ dataset under the out-of-distribution setting, as it should be enough to demonstrate the robustness of our method. The performance of the different values of these hyperparameters is plotted in Fig. C.16. From this figure, we can observe that our proposed method is not sensitive to the selection of hyperparameters and all the results are superior to the baseline methods.

## Appendix D. Running Examples

**Example of PBPS.** To better understand the workflow of PBPS, we have also added some numerical examples to illustrate visually as shown in Fig. C.17. From the figure, we inspect what has happened inside the PS/PBPS when the symptom ‘moist rales’ is inquired about. The previous patient simulator PS simply searches the symptom in the anchor record and returns ‘not sure’ when the symptom is not found. As for PBPS, when the symptom is not found in the record, PBPS matches other records with the same disease according to their propensity scores and assigns weights to matched records according to the similarities. And finally, the symptom existence is sampled according to the similarity weights. From the example, we can see that the propensity of ‘non-inquired’ is about 1.0 for the symptom ‘moist rales’. This also reflects that the

Table C.7: The statistical characteristics of the human evaluation of different participants.

Participant ID	1	2	3	4	5	6
NT (MZ)	0.82±0.38	1±0	1±0	0.90±0.31	1±0	0.62±0.49
SDC (MZ)	0.94±0.24	1±0	1±0	0.90±0.31	1±0	0.81±0.39
NT (DX)	0.52±0.50	1±0	1±0	0.68±0.47	1±0	0.69±0.46
SDC (DX)	0.89±0.31	0.96±0.20	1±0	0.86±0.35	1±0	0.85±0.36

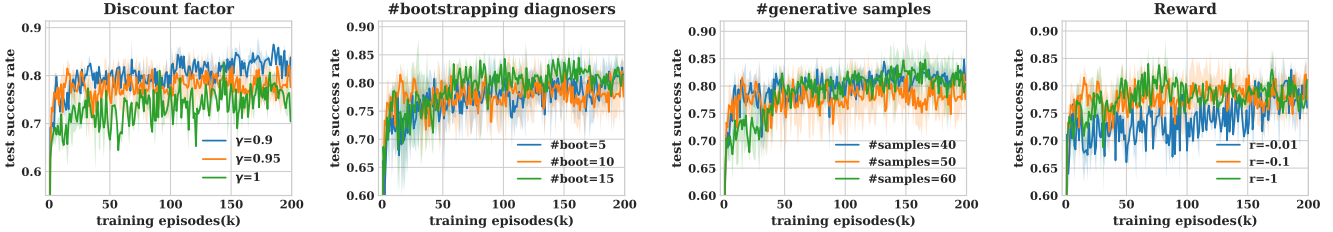


Figure C.16: The success-rate curves of our P2A across different hyperparameters on MZ under Out. setting. From left to right, the figures are for different discount factors, the number of bootstrapping diagnosers, the number of samples of bootstrapping diagnosers, and rewards. The curves of the default hyperparameters are orange.

Table C.8: The statistical hypothesis testing (P-value) of different hypotheses.

Hypothesis	NT (MZ)	SDC (MZ)	NT (DX)	SDC (DX)
P-value	5.4e-21	1.2e-33	9.0e-20	1.6e-47

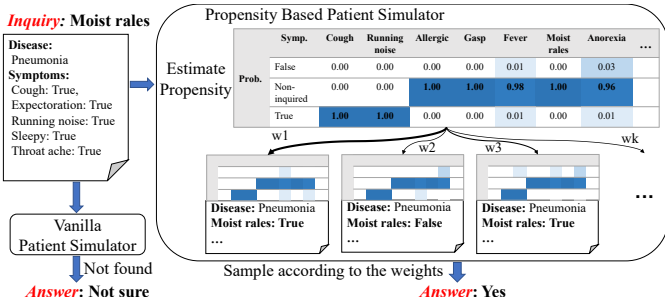


Figure C.17: A running example of PBPS. The vanilla patient simulator can only answer counterfactual symptom inquiries with ‘not sure’ words. PBPS calculates the similarity weights of other records according to the propensity scores and then it samples an answer from one of the similar records.

<b>Disease:</b> Upper tract Infection	Symp.	Sneeze	Gasp	Moist rales	Sleepy	Rhinobyon	Anorexia	...
<b>Symptom:</b> Cough: True	False	0.00	0.00	1.00	0.52	0.06	0.00	
Running Noise: True	True	1.00	1.00	0.00	0.48	0.94	1.00	
Expectoration: True								
Fever: False								
<b>Disease:</b> Pneumonia	Symp.	Sneeze	Gasp	Moist rales	Rhinobyon	Anorexia	Headache	...
<b>Symptom:</b> Cough: True,	False	0.00	0.00	0.03	0.00	0.30	0.37	
Expectoration: True								
Running noise: True								
Sleepy: True,	True	1.00	1.00	0.97	1.00	0.70	0.63	
Throat discomfort: True								

Figure C.18: Answer probabilities of several counterfactual symptom inquiries of PBPS w.r.t. two different diagnosis records. Both of the records have respiratory diseases and therefore they have many symptoms in common. However, PBPS captures the critical and distinguishable symptom, i.e., ‘moist rales’, between these diseases.

patient simulators like PS and GEN are likely to answer with “not sure”.

When inspecting the probabilities of answers to different symptom inquiries by PBPS, we found an interesting case as bounded by the red box in the tables of Fig. C.18. We found that between the two cases with respiratory diseases, i.e., “upper tract infection” and “pneumonia”, the probabilities of “moist rales” differ toward two opposite extremes when the others are closed. Moist rale is a symptom that happens in the lung which is positioned in the lower tract. Therefore, the upper tract infection certainly does not include moist rales. The doctor can easily exclude the upper tract infection if the patient has moist rales. However, there is still a small chance (0.03) that the patient with pneumonia would not have moist rales. For example, if the secretions are little and almost existed in the alveolar cavity of the pneumonia patient, the doctor usually could not hear the moist rales. Although the moist rale is distinctive, the previous simulated patient with the upper tract infection will answer with “not sure” in 99.18% of the time, because the moist rales in 99.18% of the records with the upper tract infection are not non-inquired.

**Example of P2A.** To intuitively demonstrate our P2A, Fig. C.19 is an intermediate running example. This figure shows the working pipeline of our framework from the beginning and in the end. At each turn, P2A infer the possible complete symptoms from the observed, and then it conducts do-operation to the non-inquired symptoms. After that, the observed and the estimated symptoms are fed to several bootstrapping diagnosers to estimate the diagnostic probabilities and confidences. If the decision threshold is not met, P2A will continue inquiring. Otherwise, it stops to inform disease. This example shows that P2A is unconfident in the beginning and becomes very confident in the end. To keep the example in brief, we don’t draw the complete process here and more numerical results of this example have been summarized in Fig. D.20.

In Fig. D.20, it consists of the anchor record and a series of interaction items. The interaction item at each time point includes the output of the patient simulator PBPS,

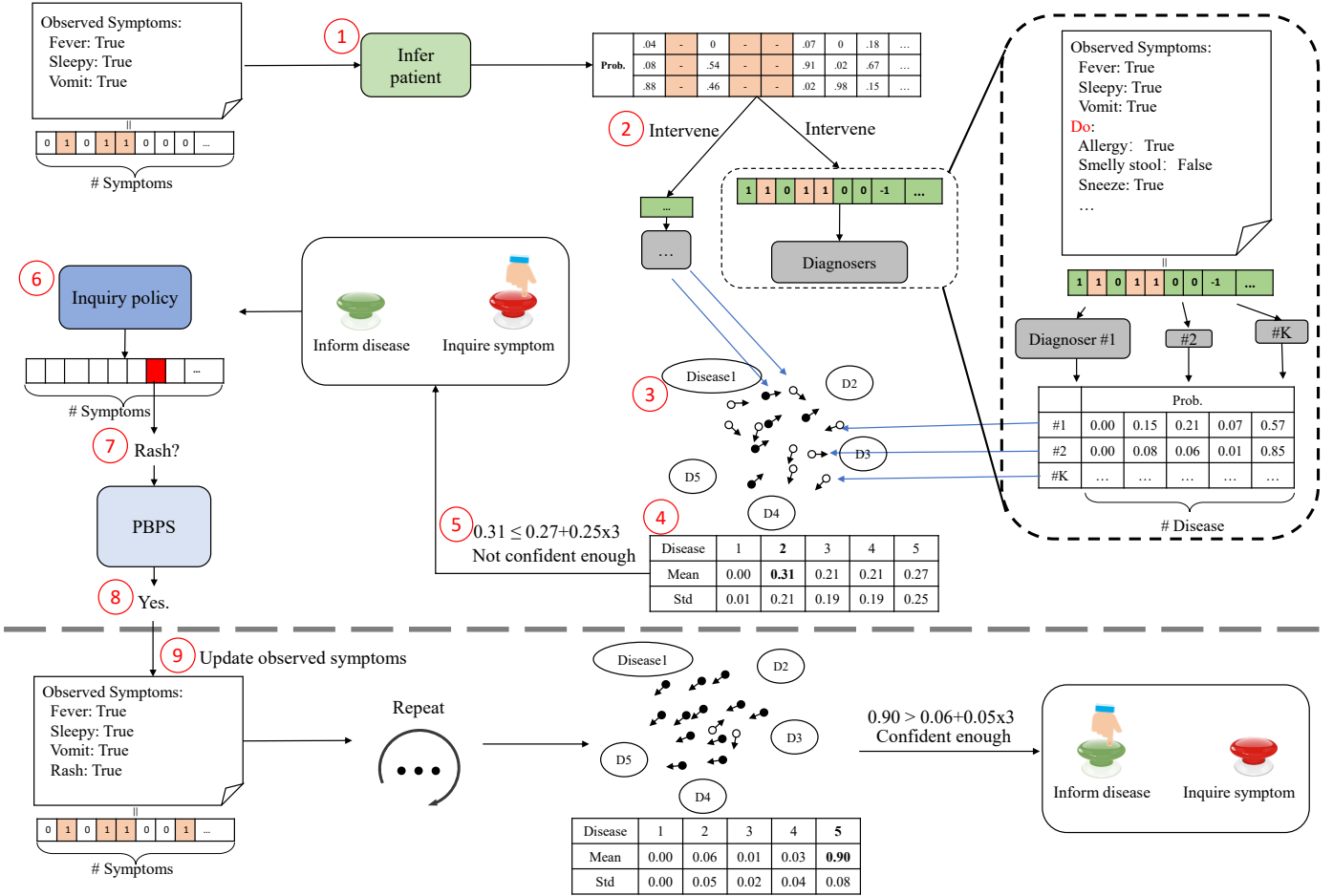


Figure C.19: A running example of P2A. For better understanding, we mark the execution order with red circled numbers. The diagnosis branch takes  $s_t^p$  to draw  $K$  final states which are fed into the  $B$  bootstrapping diagnosers to obtain the expectation and deviation. P2A keeps inquiring about symptoms of the patient simulator until the diagnosis meets the decision threshold.

the mentioned symptoms, the estimated disease expected probability and standard deviation, whether the decision threshold is met, and the actual action of the agent P2A. As shown in Fig. D.20, at the beginning, the patient simulator reported its explicit symptoms to the agent, according to which the agent predicted that upper respiratory tract infection is the most likely disease. But the agent also foresaw the future variables and its decision threshold suggested that the disease could also be infantile diarrhea if some relevant symptoms were presented. As a result, our agent was required to keep inquiring, and during diagnosing, the most likely disease was also changing. Finally, when the decision threshold was reached, the agent made a confident and correct diagnosis. This example shows that simply rendering the most likely disease without considering the future possibilities can lead to reckless and erroneous results. In addition, from the perspective of the patient simulator, we can also observe that the set of implicit symptoms is empty in the anchor record. Therefore, if the agent were interacting with the original patient simulator, it cannot obtain useful information.

However, our method also has side effects, as shown in Fig. D.21. We observe that though the agent first esti-

mates correctly based on the explicit symptoms, the agent is forced to query too many symptoms for meeting the decision threshold. Consequently, the dialogue became over-length. These two examples can also be seen in the real-life decision-making process. Sometimes a person is called cautious and responsible when making a decision rationally, while sometimes the same person is called wandering and indecisive when thinking too much and missing the opportunities. Although most of the time, people don't want to be indecisive. But as for medical applications, if a MAD agent is hesitant, it is always better not to make a decision and seek experts for help than to make a wrong decision recklessly.

Record									
<b>Self-report:</b> "Hello, doctor, my boy is one-year-old. Normally, he had two or three stools per day. Yesterday, he had four stools. I didn't take it seriously because he looked not bad. He had two stools this morning with large amount The stools were yellow and a little bit white. He vomited after drinking milk (the amount of milk was only half of that in normal times) and had a low fever of 38.1. He is in a bad looking and sleepy. He had two stools in the afternoon. He is not willing to drink milk and water. How should I care for him? Should I take him to the hospital?"; <b>Disease_tag:</b> Infantile diarrhea; <b>Explicit_inform_slots:</b> ['fever': True, 'sleepy': True, 'vomit': True]; <b>Implicit_inform_slots:</b> []									
Disease probabilities (Upper line) & standard deviation (Lower line)									
Time	PBPS	State tracker	Rhinal- ltergosis	upper respiratory tract infection	pneumonia	Infantile hand foot mouth	Infantile diarrhea	Satisfy decision threshold?	Action
0	Self-report	['fever': True, 'sleepy': True, 'vomit': True]	0.003 0.006	<b>0.306</b> 0.208	0.209 0.192	0.209 0.189	0.273 , 0.249	$0.306 \leq 0.273+0.249*3$ , No	"Does he have rash?"
1	"Yes, he has"	[..., 'rash': True]	0.004 0.010	0.134 0.178	0.182 0.170	<b>0.546</b> 0.287	0.134 0.199	$0.546 \leq 0.134+0.199*3$ , No	"Does he have herpes?"
2	"Yes, he has"	[..., 'herpes': True]	0.010 0.038	0.176 0.139	0.167 0.169	<b>0.401</b> 0.237	0.245 0.233	$0.401 \leq 0.245+0.233*3$ , No	"Does he have moist rale?"
3	"I am not sure"	[..., 'moist rale': not-sure]	0.009 0.018	0.189 0.153	0.161 0.150	<b>0.420</b> 0.242	0.221 0.227	$0.420 \leq 0.221+0.227*3$ , No	"Does he have oliguria?"
4	"I don't know"	[..., 'oliguria': not-sure]	0.001 0.001	<b>0.524</b> 0.244	0.021 0.036	0.063 0.085	0.391 0.267	$0.524 \leq 0.391+0.267*3$ , No	"Does he have loose stool?"
5	"Yes, he has"	[..., 'loose stool': True]	0 0	0.247 0.0180	0.020 0.026	0.034 0.050	<b>0.698</b> 0.204	$0.698 \leq 0.247+0.180*3$ , No	"Does he have egg pattern stool?"
6	"Yes, he has"	[..., 'Egg pattern stool': True]	0 0	0.059 0.045	0.016 0.020	0.028 0.043	<b>0.897</b> 0.081	$0.897 > 0.059+0.045*3$ , Yes	"He might have infantile diarrhea."

Figure D.20: A correct diagnosis example of our methods on DX. As the diagnosis progresses, the expected disease is changing accordingly, and finally, the correct diagnosis is made with DT satisfied.

Record									
<b>Self-report:</b> "My eight month old baby has a red rash on his back, chest and feet. His mental state is OK. At about 3 p.m., he had a fever, and the gun was 37.5. His eyes were red and swollen. From this morning to noon, he had three loose stools. Just at half past five, he had another watery one. What should I pay attention to, Dr. Zhang?"; <b>Disease_tag:</b> Infantile diarrhea; <b>Explicit_inform_slots:</b> ['fever': True, 'rash': True, 'loose stool': True, 'red eye': True]; <b>Implicit_inform_slots:</b> ['sleepy': False]									
Disease probabilities (Upper line) & standard deviation (Lower line)									
Time	PBPS	State tracker	Rhinal- ltergosis	upper respiratory tract infection	pneumonia	Infantile hand foot Mouth	Infantile diarrhea	Satisfy decision threshold?	Action
0	Self-report	['fever': True, 'rash': True, 'loose stool': True, 'red eye': True]	0.068 0.116	0.192 0.191	0.028 0.048	0.305 0.289	<b>0.407</b> 0.306	$0.407 \leq 0.305+0.289*3$ , No	"Does he have moist rale?"
1	"I am not sure"	[..., 'moist rale': not-sure]	0.099 0.192	0.165 0.165	0.039 0.067	0.308 0.287	<b>0.389</b> 0.283	$0.389 \leq 0.308+0.067*3$ , No	"Does he have herpes?"
2	"Yes, he has"	[..., 'herpes': True]	0.092 0.145	0.171 0.149	0.046 0.065	0.205 0.226	<b>0.486</b> 0.276	$0.486 \leq 0.205+0.226*3$ , No	"Is he allergy?"
3	"I don't know"	[..., 'allergy': not-sure]	0.066 0.117	0.227 0.167	0.030 0.035	0.240 0.229	<b>0.436</b> 0.278	$0.436 \leq 0.240+0.229*3$ , No	"Does he have oliguria?"
-	-	-	-	-	-	-	-	No	-
13	"Yes, he does"	[..., 'night sweat': True]	0.143 0.171	0.127 0.125	0.043 0.053	0.040 0.059	<b>0.647</b> 0.235	$0.647 \leq 0.143+0.171*3$ , No	"Does he has asthma?"

Figure D.21: A diagnosis example without satisfying DT produced by our methods on DX. The disease is correctly estimated at the very beginning but the agent is forced to query more symptoms in order to meet DT. The most likely diseases of items (from Time 4 to Time 13) are still 'Infantile diarrhea', therefore, we omitted them to keep the demonstration brief.